PERFORMANCE EVALUATION OF INNOVATIVE TOGGLE BRACE DAMPER FOR FLEXIBLE STRUCTURE SEISMIC UPGRADE
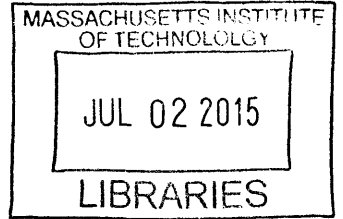
by

Jian Hua Jiang

B.A.Sc Civil and Environmental Engineering
University of British Columbia, 2013

Submitted to the Department of Civil and Environmental Engineering in Partial
Fulfillment of the Requirement for the Degree of

MASTER OF ENGINEERING IN CIVIL AND ENVIRONMENTAL ENGINEERING
at the

MASSACHUSETTS INSTITUTE OF TECHNOLOGY

JUNE 2015

Signature of Author:.................... **Signature redacted**

Department of Civil and Environmental Engineering
May 15, 2015

Certified By:........................... **Signature redacted**

Jerome J. Connor
Professor of Department of Civil and Environmental Engineering
Thesis Supervisor

Certified By:..................... **Signature redacted**

Pierre Ghisbain
Lecturer, Department of Civil and Environmental Engineering
Thesis Supervisor

Certified By:........................... **Signature redacted**

Heidi M. Nepf
Donald and Martha Harleman Professor of Civil and Environmental Engineering
Chair, Department Committee for Graduate Students

PERFORMANCE EVALUATION OF INNOVATIVE TOGGLE BRACE DAMPER FOR FLEXIBLE STRUCTURE SEISMIC UPGRADE

by

Jian Hua Jiang

Submitted to Department of Civil and Environmental Engineering on May 15, 2015
In Partial Fulfillment of the Requirements for the Degree of
Master of Engineering in Civil and Environmental Engineering

ABSTRACT

Amplifying the motion of viscous dampers has been recognized as an effective solution to mitigate structural response to wind and seismic excitation. Motion amplification devices are designed to amplify a small interstory drift to intensify the stroke of the dampers attached. The efficiency of such devices relies on their geometric configurations in addition to the stiffness of the support elements. This thesis focuses on the seismic performance evaluation of the toggle brace frame configuration employed for seismic upgrade.

In order to carry out a performance evaluation of the toggle brace damper, a practical approach to performance-based earthquake engineering (PBEE) is presented in this study. The approach considers the seismic hazard, structural response, resulting damage, and repair costs associated with restoring the building to its original condition using a fully probabilistic analysis. The procedure is organized to be consistent with conventional building designs, construction, and analysis practices so that it can be readily incorporated into a design process.

A nine-story moment frame located in downtown Los Angeles based on pre-Northridge design code is subjected to PBEE evaluation in this study. The performance of the structural frame is assessed by conducting a non-linear dynamic time history analysis in both cases, with and without the inclusion of the toggle brace damper. The results and comparisons are detailed in the chapters of this thesis.

Thesis Supervisor: Jerome J. Connor
Title: Professor of Civil and Environmental Engineering
Thesis Supervisor: Pierre Ghisbain
Title: Lecturer, Civil and Environmental Engineering

ACKNOWLEDGEMENTS

My time at Massachusetts Institute of Technology has been filled with interesting and challenging course work for both within and outside of my major. I would like to take this opportunity to express my gratitude for many who have supported me during my studies in MIT. First and foremost, I would like to thank my advisor Professor Jerome J. Connor, who has taught me many aspects of motion based design and has introduced me to this topic of toggle brace damper. I would also like to thank Dr. Pierre Ghisbain, for his excellent mentorship and support during the production of this thesis.

I would also like extend my acknowledgements to my best friend at Harvard University, Bicheng Han, and my colleagues at MIT, Isabelle Wenting Su, Linyi Zou, Junjiao Gan, for their supports, encouragements, and entertainments during the writing of this thesis.

Lastly, special thanks are dedicated to my mother, Ms. Shuxia Zhan, my uncle, Mr. Liguang Zhan, my sister, Ms. Biling Zhan, and my family. I thank them for their love, support, encouragement, and most of all their believe in me.

TABLE OF CONTENTS

LIST OF FIGURES

LIST OF TABLES

CHAPTER 1: INTRODUCTION

Traditional design of seismic force-resisting system typically follows the equivalent static force procedure (ESFP). In this design procedure, parameters are firstly designed using code-specified spectral acceleration, assuming the structures to behave elastically. In order to compensate for the structures ability to deform inelastically, base shear is reduced by a reduction factor R, design forces are adjusted using an occupancy importance factor, and drift at corresponding design forces are multiplied by a deflection amplification. However, structures based on the code design usually experience large unpredictable inelastic deformation during major earthquakes. Some of these structures experienced dramatic damages during some of the major earthquakes in the early 90s in the Los Angeles area. One of the challenging task nowadays is to retrofit and seismically upgrade these buildings, so that they can serve up to their design life. Addition of stiffness to an existing system would be difficult and counter productive; hence, it is a common practice to introduce damping mechanism into an existing system. To effectively provide sufficient damping to limit inter-story drifts, structural engineers are developing new configurations of damper geometry set-ups. Different measures to upgrade existing structural systems for such structures were proposed; it is proven to be more effective to provide additional damping mechanisms for these structures (Zhao & Chan, 2014). Energy dissipation systems with viscous dampers have been recognized as effective solutions to mitigate wind and seismic excitation for existing structures. This is because viscous dampers have proved to be a very effective device to dissipate large amounts of energy from earthquake and wind in order to maintain the structural response within acceptable limits. These devices are ideally suited for flexible structures such as moment frames (Raju, Prasad, Muthumani, Gopalakrishnan, Iyer, & Lakshmanan, 2011).

To properly examine the effectiveness of using toggle brace to seismically upgrade existing under-performing moment frames, a series of analytical studies has been conducted to study the system response of the toggle brace frame. First, the hysteresis behaviour of the toggle brace frame has been researched. The researched data were used to calibrate an analytical brace model in SAP2000. The calibrated analytical brace model was then used in a SAP2000 structural model to evaluate the system response of the toggle brace frame.

The merits of this study lie in the following points:

1. An innovative structural system, the toggle brace frame, has been studied.
2. Computer simulation has been conducted. This simulation accounts for the geometry and material nonlinearity in the analytical elements to study the system response of a complex structural system, in this case the addition of toggle brace frame to an existing moment frame.
3. A performance evaluation methodology has been used. The methodology consistently accounts for the inherent uncertainties in the ground motion, model, damage, and repair action to compute a quantitative probabilistic description of the seismic risk of the structure.
4. The methodology has been implemented in an end-to-end computer program, which engineers can use to evaluate the structural performance of different structural framing systems.

The following subsections provide additional discussion on each of these three elements.

1.1 TOGGLE BRACE FRAME

The toggle brace frame configuration (Figure 1) was first proposed by Constantinou (Constantinou, Tsopelas, Hammel, & Sigaher, 2001). The frame has geometry similar to that of conventional braced frame, except that a freely rotational pin in the middle of the brace separates the diagonal brace into two pieces. The two separated pieces do not lie in the same line, a third piece of brace element containing a damper is one end attached to the end of the brace with the other end attached to the corner of a frame. Unlike conventional diagonal brace frame, the toggle brace frame is not very effective in providing stiffness to limit the story drifts. However, it is very effective in providing damping for energy dissipation for wind and seismic. Hence, it is ideal to seismically upgrade existing under-performing moment frames structures.

12
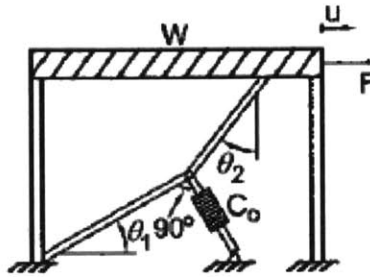
Figure 1 Configuration of Lower Toggle Brace Setup (Constantinou, Tsopelas, Hammel, & Sigaher, 2001)

In the event of severe earthquake shaking, the drift that occurred in the first few story is the greatest for moment frame. If the drift is so great that it exceeds the elastic range of the moment frame, hinges will form in either the ends of a column or either ends of a beam. There will be a high probability of collapse for when plastic hinges form in the column due to loss of lateral stiffness.

Building structures respond to dynamic excitation with some interstory drifts, floor velocities, and floor accelerations. The practice of implementing damping devices as diagonal elements leads to damping device displacement less than the drift. This, in turn, results in the requirement for substantial forces in the damping devices for effective energy dissipation. On the basis of this consideration, it appears that to effectively improve an existing structural system, we need to geometrically amplify the local displacement of the damper. Toggle brace frame, magnifies the motion of the damper in the range of about 2.5 – 5 times the interstory drift (Li & Liang, 2008), Allowing a much lower damping force for effective energy dissipation.

1.2 PROBABILISTIC SEISMIC PERFORMANCE ASSESSMENT

The framework for performance-based assessment, developed by the Pacific Earthquake Engineering Research Center (PEER), provides the means to consistently account for the inherent uncertainties in ground motion, structural response, structural damage occurrence and distribution, and their repair procedures and cost to give building owners/stakeholders performance metrics that can be used to make risk management decisions. A new method for generating consistent structural demand measures was researched and implemented to enable the

13

application of the PEER framework to the seismic evaluation of the toggle brace frame. The method samples the structural response from a few dynamic analyses and generates additional correlated response matrix using functions of random variables (Applied Technology Council, 2012). With the generated correlated response matrix the performance of the structural system was assessed using the Monte-Carlo simulation. An end-to-end computer implementation of the new method was used to conduct a comparative seismic performance assessment of a SAC pre Northridge moment frame before and after the addition of a toggle brace frame.

1.3 RESEARCH OBJECTIVES

The first objective is to develop a base-line understanding of the hysteresis behaviour of the toggle brace frame through literature review and to conduct a study of the behavior of different configurations of toggle brace frames. This study can aid understanding how the damping forces distribute in the system.

The second objective is to examine how much interstory drifts and floor accelerations are reduced in an existing moment frame prototype by adding toggle braces into the system.

The third objective is to develop an implementation of the PEER probabilistic performance-based seismic evaluation of structural framing systems. Traditional performance evaluation of structural framing systems uses performance objectives defined in terms of structural response measures such as story drift or floor acceleration. While such response quantities are useful in providing indirect performance measures, many decision makers prefer performance metrics that more directly relate to business decisions, such as downtime and repair costs. The implementation of the PEER probabilistic performance-based seismic evaluation framework developed in this study will enable engineers to compute performance in terms of capital losses, and thereby help inform decisions about design levels within a risk management framework (Hunt & Stojadinovic, 2010). This implementation will be used to evaluate the performance of the toggle brace frame when they are added to an existing moment frame.

14

CHAPTER 2: ANALYTICAL STUDY OF STEEL TOGGLE BRACE

2.1 BRIEF THEORY ON TOGGLE-BRACE

For the configuration of diagonal and chevron brace, the displacement of the energy dissipation devices is either equal to or less than the drift of the story at which the devices are installed. We can use u_D to denote displacement of the damper, u to denote the interstory drift, and f to denote the magnification factor. We can develop the following relationship:

$$u_D = f \cdot u$$ Equation 1

For the chevron brace configuration, $f = 1.0$, whereas for the diagonal brace configuration, $f = cos\theta$, where θ is the angle of inclination of the damper (see Figure 2).

The force alone the damper, denoted by F_D, is similarly related to the horizontal component of force, F

$$F = f \cdot F_D$$ Equation 2

Figure 2 illustrates the diagonal and chevron brace configuration and the force F and interstory drift u for a single-story structure has effective weight W and a fundamental period (for elastic conditions) T, and that it is equipped with a fluid linear viscous damper for which

$$F_D = C_D \cdot \dot{u}_D$$ Equation 3

where C_D is the damping coefficient, and $\dot{u}_D$ is relative velocity between the ends of the damper along the axis of the damper. Damping ratio can be calculated as

$$\zeta = \frac{C_D \cdot f^2 \cdot g \cdot T}{4 \cdot \pi \cdot W}$$ Equation 4

The significance of the configuration of the energy dissipator is clear by looking at the magnification factor. A damper selected to provide a damping ratio of 5% in the chevron brace can only provide a damping ratio of 3.2% in the diagonal configuration (Hwang, Huang, Yi, & Ho, 2008).

| Diagonal | | $f = cos\theta$ | $\theta = 25^o$
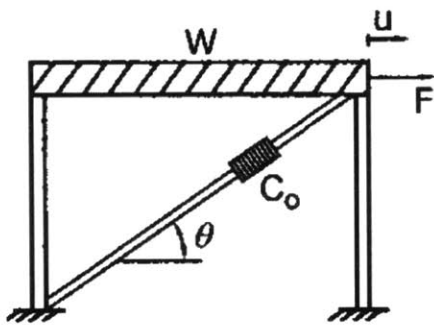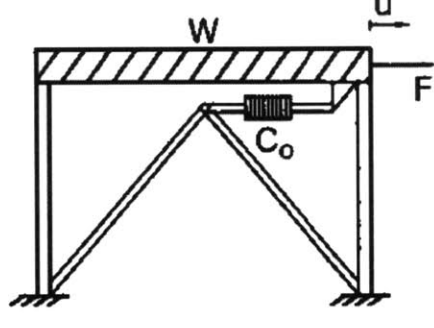
 $f = 0.91$ |
| Chevron | | $f = 1.0$ | $f = 1.0$ |

Figure 2 Illustration of diagonal and chevron brace configurations and magnification factors (Constantinou, Tsopelas, Hammel, & Sigaher, 2001)

To further examine the effectiveness of a toggle brace, it is meaningful to look at the magnification factors it provides in comparison to diagonal or chevron brace damper systems.

The magnification factor, f, is the ratio of the damper displacement, u_D, to the interstory drift, u.

$$f = \frac{u_D}{u} = \frac{|\overline{A'B'} - \overline{AB}|}{u}$$

Equation 5

By neglecting any axial deformation with the brace elements, the displacements of the dampers of upper and lower toggle dampers (shown in Figure 3) can be established as follows (Constantinou, Tsopelas, Hammel, & Sigaher, 2001):

- For the upper toggle system

$$u_D = \pm \left\{ \frac{h}{\cos \theta_1} - l_1 \cdot \tan \theta_1 - \left[\left(h \cdot \tan \theta_1 - u - \frac{l_1}{\cos \theta_1} + l_1 \cdot \cos(\theta_1 \pm \phi) \right)^2 + (h - l_1 \cdot \sin(\theta_1 \pm \phi))^2 \right]^{1/2} \right\}$$

Equation 6

- For the upper toggle system

$$u_D = \pm l_1 \cdot \left[\left(1 + \frac{1}{\cos^2 \theta_1} - \frac{2 \cdot \cos(\theta_1 \pm \phi)}{\cos \theta_1} \right)^{1/2} - \tan \theta_1 \right]$$

Equation 7

17
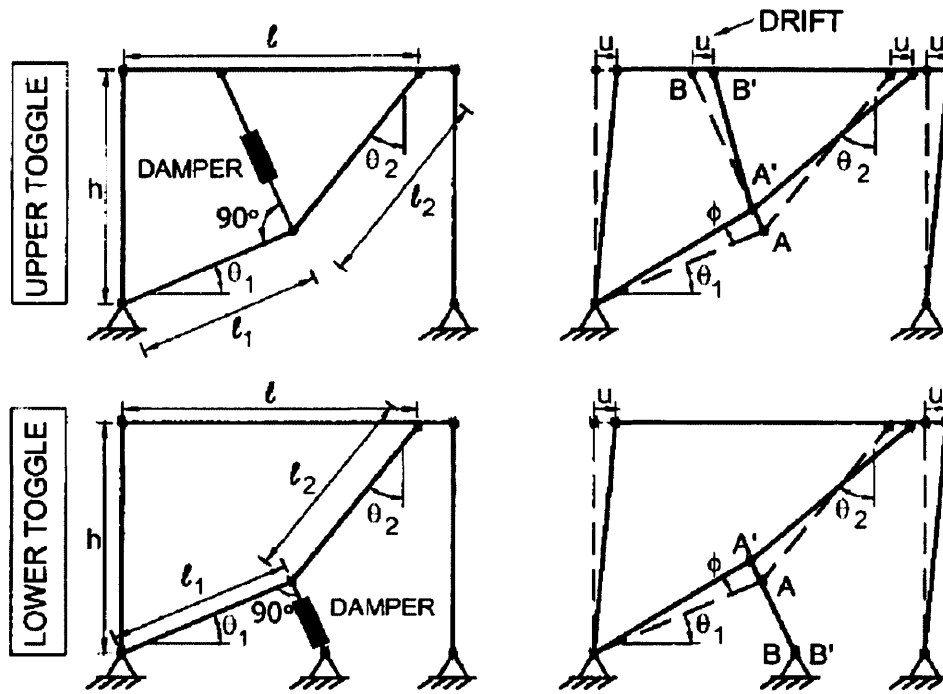
Figure 3 Upper and lower toggle brace displacement (Constantinou, Tsopelas, Hammel, & Sigaher, 2001)

In the above equations, positive drift u and rotation ϕ are as shown in Figure 3. The relationship between the damper displacement and drift for the toggle brace damper is shown in Equation 6 and Equation 7. The simple magnification factor can be obtained by retaining only the linear terms in ϕ and u (Constantinou, Tsopelas, Hammel, & Sigaher, 2001). The result is:

- For the upper toggle system

$$f = \frac{\sin \theta_2}{\cos (\theta_1 + \theta_2)} + \sin \theta_1 \qquad \text{Equation 8}$$

- For the lower toggle system

$$f = \frac{\sin \theta_2}{\cos (\theta_1 + \theta_2)} \qquad \text{Equation 9}$$

18

2.2 FORCE IN TOGGLE BRACE SYSTEM

By solving equilibrium, axial forces in the toggle are as follows (Hwang, Huang, Yi, & Ho, 2008):

$$T_1 = F_D \cdot \tan(\theta_1 + \theta_2)$$
Equation 10

$$T_2 = \frac{F_D}{\cos(\theta_1 + \theta_2)}$$
Equation 11

$$T_3 = \frac{\alpha \cdot F_D}{\cos(\theta_1 + \theta_2)}$$
Equation 12

$$T_4 = \alpha \cdot F_D \cdot \tan(\theta_1 + \theta_2)$$
Equation 13

Where the forces T_1 and T_2 are tensile, T_3 and T_4 are compressive, as shown in Figure 4.

The following force-displacement relationship can be developed by looking at the magnification factor:

$$f = \frac{F}{F_D} = \frac{u_D}{u} \implies F_D \cdot u_D = F \cdot u$$
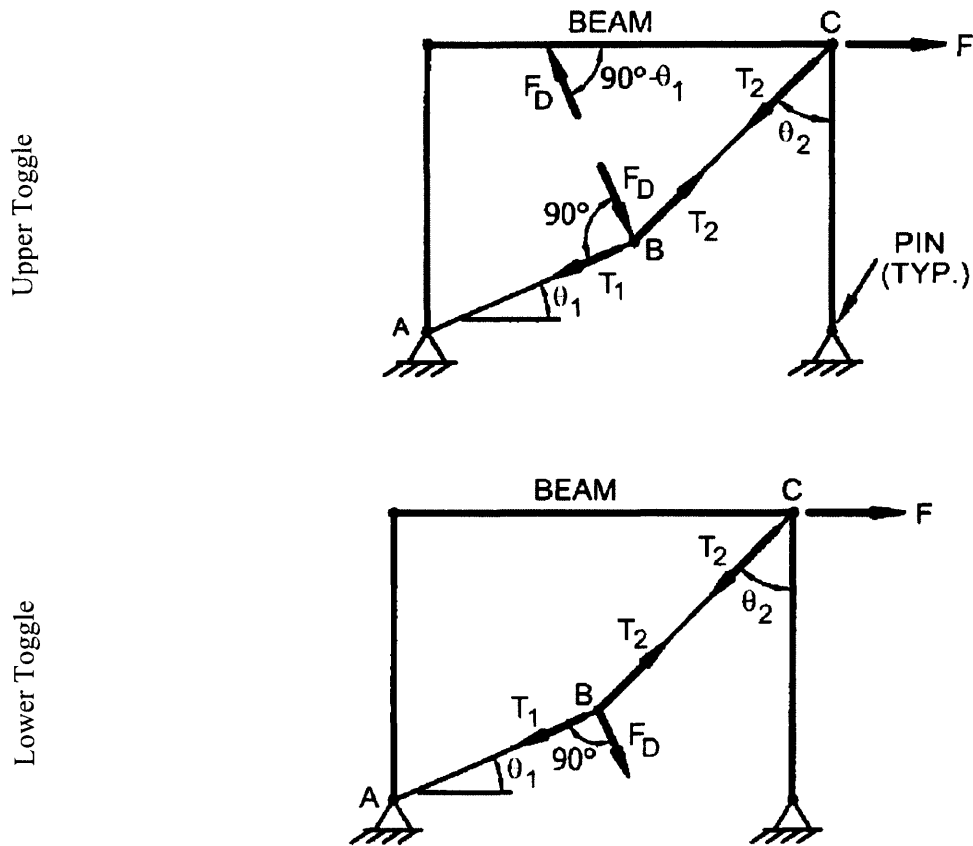
Figure 4 Toggle Brace system force diagrams (Hwang, Huang, Yi, & Ho, 2008)

2.3 DESIGN PROCEDURE FOR TOGGLE BRACE DAMPER SYSTEM STRUCTURES

Since design procedures for structure with toggle brace damper (TBD) systems are not provided in codes, a proposed design procedure (Li & Liang, 2008) is adopted in this research. This procedure is a simplified procedure for seismic design and analysis of structure with the improved TBD system to determine the effective damping ratio that limit the drift of the damped structure to the specified value. The detail of the steps is as follows:

1) Specify the limiting value of interstory drift, Δ, for a structure with the toggle brace damper for the given earthquake intensity level.

20

2) Determine the velocity exponent range for viscous damper from 0.35 to 1 (Li & Liang, 2008).

3) Evaluate the total effective damping ration ζ_{eff}, according to the assumed the supplemental equivalent viscous damping ratio, ζ_d.

4) Calculate the roof displacement based on response spectrum calculation $D_i = \Gamma_1 \cdot S_d(T_1, \zeta_{eff})$, where Γ_1 is the participation factor of the first mode shape normalized to unit value at roof level, and S_d is the spectra displacement depending on the fundamental natural period T_1 and the total effective damping ratio ζ_{eff} that is assumed in the step 3).

5) Compute the maximum interstory drift expressed as, $\Delta_{max} = D_i \phi_{i,max}$, where $\phi_{i,max}$ is the maximum modal interstory drift.

6) If the estimated maximum interstory drift, Δ_{max}, obtained from step 5) is less than the limiting interstory drift, Δ, go to step 7); otherwise,

   let $\zeta_{eff, \ new} = \frac{\Delta_{max}}{\Delta} \cdot \zeta_{eff}$ and repeat step 3) to 6).

7) Determine the damping coefficient of damper distributed over the height of the structure according to Equation 4.

8) Check the actions for components of the building using static method of analysis at the stage of maximum displacement, maximum velocity and maximum acceleration.

Based on the toggle brace damper design procedure proposed by Li and Liang, a ζ_{eff} value of 12% is determined for the upgrade of the SAC nine-story pre-Northridge design, detail analysis results can be found in the Chapter 4 of this thesis.

CHAPTER 3:   PERFORMANCE-BASED METHODOLOGY FOR EVALUATING STRUCTURAL FRAMING SYSTEMS

Earthquake engineering has evolved from using a set of prescriptive provisions, indirectly aimed at providing life safety, to performance-based approaches with direct consideration of a range of performance objectives. Performance-based approaches have several advantages, including a more comprehensive consideration of the various performance metrics that might be of interest to stakeholders, more direct methods for computing performance, and an increasing involvement of stakeholders in decisions on design acceptability. Whereas engineers are familiar with performance measures such as drift, acceleration, strain, and perhaps damage state, many decision-makers prefer performance metrics that related more directly to business decisions, such as downtime or repair costs. An engineering challenge has been to consistently consider seismic hazard, structural response, and resulting damage and consequences, such that a fully probabilistic statement of expected performance can be made.

A rigorous, yet practical approach to performance-based earthquake engineering (PBEE) is pursued in this chapter. The approach considers the seismic hazard, structural response, resulting damage, and repair costs associated with restoring the building to its original condition using a fully consistent, probabilistic analysis of the associated parts of the problem. The approach could be generalized to consider other performance measures such as casualties and down time, though these have not been pursued at this time. The procedure is organized to be consistent with conventional building designs, construction, and analysis practices so that it can be readily incorporated as a design approach (Moehle, Stojadinovic, Der Kiureghian, & Yang, 2005).

3.1 PERFORMANCE-BASED EARTHQUAKE ENGINEERING FRAMEWORK

To account for uncertainties in earthquake engineering problems, some prior understanding of probabilistic analysis is needed. Appendix A summarizes the basic probability theory that is used in deriving the performance-based earthquake engineering (PBEE) framework. Equation 14 shows the notation of conditional complementary cumulative distribution function

22

(CCDF) of a random variable X given the values of another random variable $Y = y$. Equation 15 shows the Total Probability Theorem for the occurrence of event A given the conditional probability of the occurrence of n mutually exclusive and collective exhaustive discrete random variables E_i.

$$G(x|y) = P(X > x|Y = y)$$

<div align="right">Equation 14</div>

<div align="right">Equation 15</div>

$$P(A) = \sum_{i=1}^{n} P(A|E_i)P(E_i)$$

Equation 15 is modified into Equation 16 to account for E being a continuous random variable. Similar to Equation 15, Equation 16 shows the total probability of event $A > a$ given event E has occurred.

<div align="right">Equation 16</div>

$$P(A > a) = \int_E P(A > a|E = de)dP(de) = \int_E G(a|e)dG(e)$$

Where de represents a small range of the continuous random variable E and the integration bound is set over the entire range of E.

3.1.1 DERIVATION OF THE PERFORMANCE-BASED EARTHQUAKE ENGINEERING FRAMEWORK

Moehle and Deierlein describe the application of Equation 16 as adopted in research of Pacific Earthquake Engineering Research Center (PEER). As implemented, Equation 16 is decomposed into four analysis steps (Yang T. , Moehle, Stojadinovic, & Der Kiureghian, 2009):

1. Seismic hazard analysis:

Probabilistic seismic hazard analysis is used to describe the seismic Hazard for the structure. The outcome of the probabilistic seismic hazard analysis is a seismic hazard curve, $\lambda(IM)$, that quantifies the annual rate of exceeding a given value of seismic

intensity measure (IM). [For example, the number of times the peak ground acceleration will exceed 0.5 g for a particular location in a given year.] In addition, seismic hazard analysis is used to characterize the ground motions that can be used in the response analysis.

2. <u>Response analysis:</u>

The response of structural and non-structural components of a building to seismic excitation is obtained using a model of the structure. This model may be analytic or physical. The ground motions used in this analysis are chosen to represent the seismic hazard range of interest for the site, and may induce inelastic response of the structure: thus, nonlinear dynamic analysis is commonly used in this step. The outcomes of response analysis are statistical functions that relate engineering demand parameters (such as interstory drift or floor acceleration) to the ground acceleration experienced by the structure.

3. <u>Damage analysis:</u>

Based on analysis of behaviour, test data, or post-earthquake reconnaissance reports, structural and non-structural damage can be characterized in terms of fragility curves. The fragility curves are cumulative distribution functions (CDFs) representing the probability that a damage state has been reached or exceeded given a quantitative measure of the engineering demand parameter (EDP).

4. <u>Loss analysis:</u>

A presentation of damage analysis results from damage quantities to decision variables that can be used by building owners and stakeholders to make a risk management decision is done during loss analysis. The outputs of the loss analysis can be, for example, the probability of exceeding a certain threshold repair cost for a set period of time or the expected monetary loss for the structure with a particular probability of exceedance.

Random variables are used to represent quantities to preserve the statistical uncertainties inherent to the problem. The seismic hazard analysis uses a probabilistic analysis of the seismic environment, ground shaking attenuation relations, and site conditions to derive a model for the seismic shaking intensity at a site. The output of the seismic hazard analysis is a statistical function that represents the annual rate of exceedance of certain intensity measures (IM), that is ,

24

$v(IM > im)$. Response analysis uses an engineering demand parameter (EDP) as the random variable and produces the conditional probability function, $G(edp|im)$, to represent the statistical relationship between *EDP* and *IM*. Damage analysis uses a damage measure (*DM*) as the random variable and the results of the analysis is a conditional probability function, $G(edp|im)$, that relates *DM* and *EDP*. Lastly, the loss analysis uses decision variable (*DV*) as the random variable and produce a conditional probability function, $G(dv|dm)$, that relates *DV* and *DM*. Figure 5 illustrates the underlying performance-based earthquake engineering framework.

Seismic Hazard Analysis $\lambda(im)$ IM: intensity measure	→	Response Analysis $G(edp|im)$ EDP: Engineering Demand Parameter	→	Damage Analysis $G(dm|edp)$ DM: Damage Measure	→	Loss Analysis $G(dv|dm)$ DV: Decision Variable
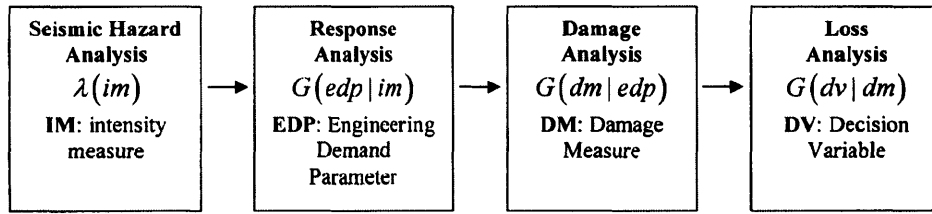
Figure 5 Perfomance-based earthquake engineering framework (Yang T. , Moehle, Stojadinovic, & Der Kiureghian, 2009)

Note that the decomposition of the PBEE process outlined above is made possible using the statistical independence assumptions listed below:

1. $G(dm|edp, im) = G(dm|edp)$ ⇐ (Conditional probability of *DM* given *EDP* and *IM* is equivalent of conditional probability of *DM* given *EDP*).

2. $G(dv|dm, edp) = G(dv|dm)$ ⇐ (Conditional probability of *DV* given *DM* and *EDP* is equivalent to conditional probability of *DV* given *DM*).

3. $G(dv|dm, im) = G(dv|dm)$ ⇐(Conditional probability of *DV* given *DM* and *IM* is equivalent to conditional probability of *DV* given *DM*).

Using the total probability theorem, the probability of exceedance for each intermediate random variable is presented in Equation 17 to Equation 19.

1. Response analysis

$$P(EDP > edp) = \int_{im} G(edp|im)dG(im) \Rightarrow dP(EDP > edp)$$

Equation 17

$$= \int_{im} dG(edp|im)dG(im)$$

2. Damage analysis

$$P(DM > dm) = \int_{edp} G(dm|edp)dG(edp) \quad \Rightarrow dP(DM > dm)$$

Equation 18

$$= \int_{edp} dG(dm|edp)dG(edp)$$

3. Loss analysis

Equation 19

$$P(DV > dv) = \int_{edp} G(dv|dm)dG(dm)$$

By conditioning Equation 19 on *im*

26

$$P(DV > dv|im) = \int_{dm} G(dv|dm, im)dG(dm|im)$$

$$= \int_{dm} G(dv|dm)dG(dm|im) \Rightarrow G(dv|im)$$

Equation 20

$$= \int_{dm} G(dv|dm)dG(dm|im)$$

By conditioning Equation 18 on *im*

$$dP(DV > dv|im) = \int_{edp} dG(dm|edp, im)dG(edp|im) = \Rightarrow dG(dm|im)$$

Equation 21

$$= \int_{edp} dG(dm|edp)dG(edp|im)$$

Substituting Equation 21 into Equation 20

Equation 22

$$G(dv|im) = \int_{dm} \int_{edp} G(dv|dm)dG(dm|edp)dG(edp|im)$$

Equation 22 represents the conditional probability of a decision variable having a value dv given a value of intensity $IM = im$. Similar derivation can be made for $G(dm|im)$ and is shown in Equation 23.

$$G(dv|im) = \int_{edp} G(dm|edp)dG(edp|im)$$

Equation 23

3.1.2 ANNUAL RATE OF EXCEEDING A THRESHOLD VALUE

$G(dv|im)$, $G(dm|im)$ and $G(edp|im)$ are the conditional probabilities of the performance measures DV, DM and EDP given an intensity measure $IM = im$. To translate the conditional probability into a quantity that can be readily used by building owners/stakeholders to make a risk management decision, these conditional probabilities are multiplied by the absolute value of the derivative of the annual rate of exceedance of a given value of the ground motion intensity measure, $\left|\frac{d\lambda(im)}{d\,im}\right|$. Because the seismic hazard curve, $\lambda(im)$, is defined as the annual rate the earthquake ground motion intensity measure IM exceeds a value im, a derivative is used to compute the annual frequency (rate of occurrence) of the intensity measure $IM = im$. An absolute value is used to ensure that this rate is a positive number regardless of the shape of the hazard curve itself.

The product of the annual rate of occurrence and the conditional probability of the performance measure given an intensity measure gives the annual rate of the performance measure exceeding a threshold value. In other words, $\left|\frac{d\lambda(im)}{d\,im}\right|$ represents the annual frequency of a random variable IM equaling im and $G(dv|im)$ represents the probability that the random variable DV takes values larger than dv for shaking intensity equalling im. Thus, their product gives the number of occurrences of $DV > dv$ annually, as shown in Equation 24.

$$\frac{\lambda(DV > dv)}{d\,im} = G(dv|im)\left|\frac{d\lambda(im)}{d\,im}\right| \qquad \text{Equation 24}$$

Integrating Equation 24 for all intensity measures, Equation 25 gives the annual rate that DV exceeds a threshold value dv for all intensity measures considered.

$$\lambda(DV > dv) = \int_{im} G(dv|im)\frac{|d\lambda(im)|}{d\,im}d\,im = \int_{im} G(dv|im)|d\lambda(im)| \qquad \text{Equation 25}$$

The final form of the performance-based earthquake engineering framing equation, Equation 26, is obtained by substituting Equation 22 into Equation 25.

28

$$\lambda(DV > dv) = \int_{im} \int_{dm} \int_{edp} G(dv|dm)dG(dm|edp)dG(edp|im)|d\lambda(im)| \qquad \text{Equation 26}$$

Note that Equation 26 uses the same conditional probability for successive earthquake events. This implies the structure is non-deteriorating or is restored to its original condition immediately after any damage to the structure occurs in an earthquake event.

3.2 AN IMPLEMENTATION OF THE PERFORMANCE-BASED EARTHQUAKE ENGINEERING FRAMEWORK

The PBEE framework described previously can be used as the basis for developing custom and rigorous PBEE procedures. The challenge is to implement the methodology in a manner that is practical for practitioners to use in a typical design office setting. Two issues must be addressed to achieve this goal (Yang, Moehle, & Stojadinovic, 2009):

The performance measures (DV, DM, and EDP) and their conditioned cumulative distribution functions, $G(x|y)$, must be easily quantified and formulated in a straightforward way using data readily available to practicing engineers

The complex computation required to integrate the PEER PBEE framework (Equation 26) must be encapsulated into procedures and routines that are transparent and easy to implement.

An implementation that fulfills these two goals is presented in the following steps:

1. Define the structural and non-structural components to be considered in the performance assessment

    The outcome of this step is a series of repair quantity tables for the structure. These tables correlate the structural and/or non-structural component damage states and repair actions needed to restore them. They are formulated using a procedure described in the following.

    Depending on the structural system and intended function of the structure, relevant structural and non-structural components of the building are selected and separated into

different performance groups (PG). Each performance group consists of one or more building components whose performance is similarly affected by a particular engineering demand parameter (*EDP*). For example, one performance group might consist of all similar non-structural components whose performance is sensitive to floor acceleration or to inter-story drift between the second and third floor. The selection of components in each performance group is based on an engineering judgment of the importance of the contribution of these components to the overall performance of the structure.

A sufficient number of damage states (*DS*) are defined for each performance group to completely describe the range of damage to the components in the performance group. The damage states are defined in relation to the repair actions needed to correct them. For each damage state, a damage model (fragility relation) is used to define the probability the component will be equal or less than the damage state given an *EDP* value. Figure 6 shows an example of Fragility curves defined for a performance group.
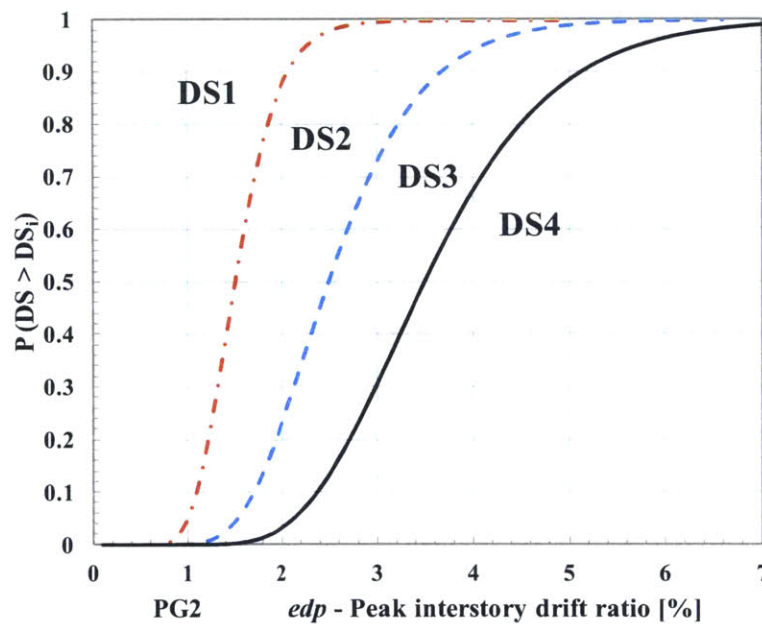
Figure 6 Example of fragility curves (Yang T. , Moehle, Stojadinovic, & Der Kiureghian, 2009)

The example fragility curves shown in Figure 6 indicate the performance group has four damage state. For example, these might be no damage (DS1), slight damage (DS2), severe but repairable damage (DS3), or damage requiring total replacement (DS4). Depending on the demand expressed using the *EDP* value, the probabilities of the performance group being in each damage state can be identified from the fragility curves. For example, if the *EDP*

being 3%, the probability of the components in the PG being in DS1 is close to zero, DS2 is approximately 0.28, DS3 is approximately 0.42, DS4 is approximately 0.3.

After the performance groups are identified, building data such as as-built documents or in-use surveys are used to quantify the components of each performance group in the building. For example, square footage of partition walls and number of pocket doors may be computed.

Because each damage state is defined according to the repair action, the total repair quantities for each item in the PG at different damage states can be defined according to the functionality of the structure. Table 1 shows an example of the repair quantities for each item in the sample performance group shown in Figure 6 at different damage states. Additional damage states and repair items can be added for different performance groups.

Table 1 Example repair quantity table for the performance group shown in Figure 6

Repair quantity type	Units	DS1	DS2	DS3	DS4
General clean-up					
Water damage	sf	0	0	10,000	20,000
STRUCTURAL					
Demolition/Access					
Finish Protection	sf	0	4,000	10,000	20,000
NON-STRUCTURAL INTERIOR					
Interior Demolition					
Remove furniture	sf	0	40,000	100,000	200,000
Ceiling sysrem removal	sf	0	0	0	500
MEP removal	sf	0	0	800	2500
Interior Construction					
Replace ceiling tiles	sf	0	3,000	9000	9000
Replace ceiling system	sf	0	0	0	20,000
MEP replacement	sf	0	0	500	2,000

2. Conduct seismic hazard analysis and ground motion selection

A conventional seismic hazard analysis is conducted, taking into account the site and the layout of the building. In practice, the hazard data would be available to engineers. One outcome of the seismic hazard analysis is a hazard curve that quantifies ground motion intensity measures considered in the PBEE analysis of the building. The hazard curve and engineering judgement are used to identify the discrete hazard levels for which the building will be further examined. Another outcome of the seismic hazard analysis is suites of ground

motions representing the seismicity of the site at different seismic hazard levels. For example, a suite of ground motions representing the seismic hazard with a 10% probability of exceedance in a 50 years at the site may be provided. A typical suite comprises several ground motions with their intensity scaled to the level implied by the seismic hazard function. The motions may be further subclasses by types, such as near-field or far-field ground motions.

3. Evaluate the response of the building

With the selected ground motions, a series of dynamic analyses, including nonlinear response if necessary, can be used to determine the earthquake response of the building. Depending on the EDP associated with each performance group (defined in step 1), the peak EDPs obtained from the dynamic analysis are summarized in an EDP matrix, X, as shown in Table 2. The columns of X represents of the different EDPs of interest. For example, EDP 1 represents second floor acceleration and EDP 2 represents third floor acceleration. The rows of X represent the peak EDPs matrix will be defined for each intensity measure considered.

Table 2 Sample EDP matrix, X

Filename	EDP 1	EDP 2	...	EDP M
Ground Motion 1	0.7	1.05	...	0.8
Ground Motion 2	0.6	0.9	...	0.5
$\vdots$	$\vdots$	$\vdots$	$\vdots$	$\vdots$
Ground Motion N	0.8	1.2	...	0.5

4. Generate additional correlated EDP vector

Computing additional EDP vector realizations using additional dynamic analysis is hampered by the paucity of recorded strong ground motions and the computational cost. Therefore, preclude running additional nonlinear dynamic analyses, a joint lognormal distribution is fitted to the EDP matrix. Correlated EDP vectors can then be generated using procedure presented in Section 3.

5. Compute the total repair cost

With the generated correlated EDP vectors, the total repair quantities for all repair items in the building after each scenario earthquake can be calculated. For a given EDP vector, the cost simulation loops through each performance group defined in Step 1. Depending on the

32

values of the *EDP* associate with performance group, a random number generator with a uniform distribution is used to select the damage state for the damage model defined in Step 1. Once the damage states are identified, the repair quantities for each item in the performance group are located from the repair quantities table, such as Table 1. This process is repeated for all performance group and the total repair quantities are summed from the quantities obtained from each performance group.

Once the total repair quantities are determined, the total repair cost for the building can be computed by multiplying the total repair quantity by the unit repair cost. Figure 7 shows an example of the unit repair cost function. The price uncertainty is represented by using a random number generator, based on the tabulated "beta" factor for the cost functions, the adjust the unit cost up or down before multiplying by the total quantities associated with each repair measure. This is the repair cost for one realization of *EDP*s. The process is repeated a large number of times to obtain a distribution of total repair cost given the hazard level. The performance groups are assumed to be statistically independent.
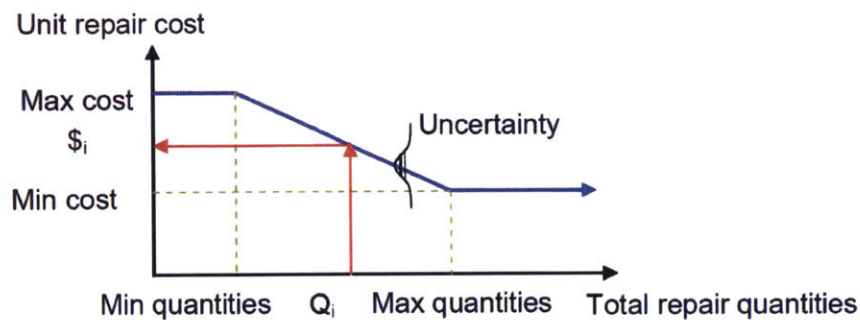
Figure 7 Example of cost function (Yang T. , Moehle, Stojadinovic, & Der Kiureghian, 2009)

6. <u>Representations and interpretations of total repair cost</u>

The methodology to obtain a total cost of the building for one intensity measure is presented from steps 1 through 5. For different intensity measures there are different distribution curves, as shown in Figure 8. These curves can be used as a basis for making risk management decisions. For example, the curve demonstrates the amount of seismic risk increase (in terms of the total repair cost) as a function of the return period of earthquake. Similar curves can be generated to compare the performance of different structural framing systems, or different retrofitting strategies on the same building.

The procedure in step 3 to step 5 have been implemented in a computer program called the Opensees Navigator. Input to the program requires the user to define the performance groups, the repair quantities table, the repair cost functions, the EDP matrices are obtained by running a limited number of response history analysis, and the total number of repair cost simulations required to compute the loss function.
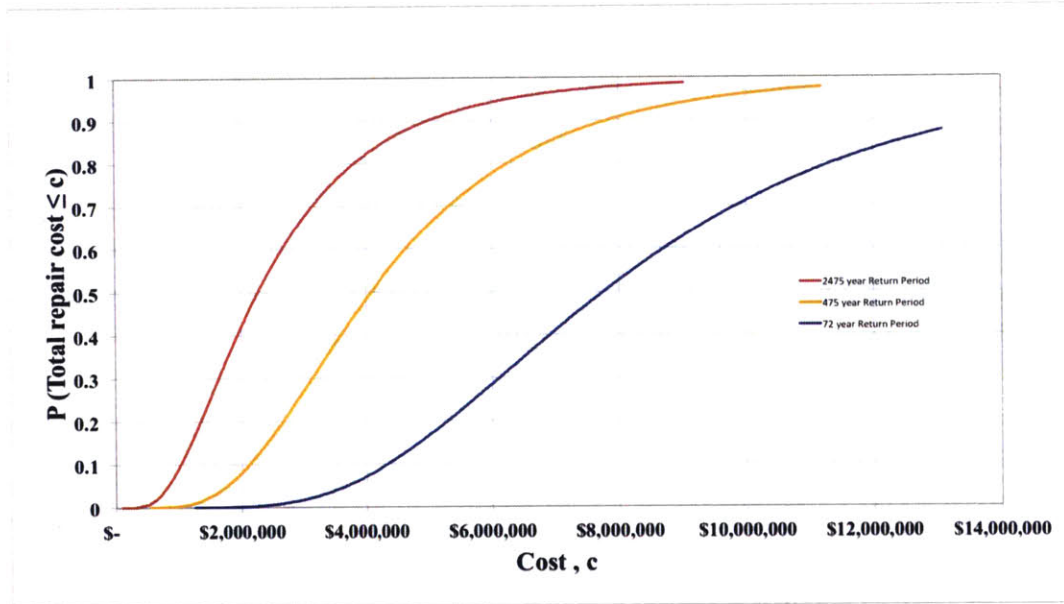
Figure 8 Sample cumulative probability distribution function for cost not exceeding a threshold value; generated according to the methodology presented above

3.3 GENERATING CORRELATED EDP VECTORS

To generate correlated EDP vectors, the peak EDP quantities recorded from sets of dynamic analysis are tabulated into matrix X, as shown in Table 2. Each column of X represents an EDP of interest, while each row of X represents different EDP recorded from a single ground motion. Because the entry of X represents the peak response quantity, a joint lognormal distribution is assumed for X.

The EDP matrix, X, is then transformed to a normal distribution, Y, by taking the natural log of X. The mean vactor, M_Y, diagonal standard deviation matrix, D_Y, and the correlation coefficient matrix, R_{YY}, are then sampled from Y. Equation 27 to Equation 30 shows the formulas

34

used for statistic sample. Detailed formulas for the statistic samples are summarized in Appendix A.

$$M_Y = [mean(Y)]^T \qquad\qquad \text{Equation 27}$$

$$D_Y = diag[std(Y)] \qquad\qquad \text{Equation 28}$$

$$R_{YY} = corrcoef(Y) \qquad\qquad \text{Equation 29}$$

$$L_Y = [Chol(R_{YY})]^T \qquad\qquad \text{Equation 30}$$

Additional correlated EDP vectors, Z, can be generated to fit the probability distribution of Y if a vector of uncorrelated standard normal distribution variables, U, with zero mean and unit standard deviation is used. Equation 31 shows the transformation from U to Z.

$$Z = AU + B \qquad\qquad \text{Equation 31}$$

Where A is a constant coefficient matrix representing the linear transformation from U to Z. B is a constant coefficient vector representing the translation from U to Z.

If U to $B = M_Y$ and $A = D_Y L_Y$, Z will have the same probability distribution as Y. Equation 32 shows the formula used to generate additional correlated EDP vectors.

$$Z = D_Y L_Y U + M_Y \qquad\qquad \text{Equation 32}$$

Finally, the generated EDP vectors are transformed to the lognormal distribution, W, by taking the exponential of Z. Figure 9 shows the process of generating correlated EDP vectors.
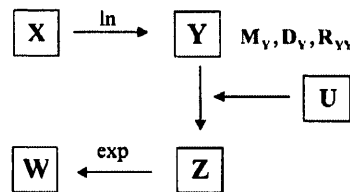
Figure 9 Process of generating the correlated EDP vectors (Yang T. , Moehle, Stojadinovic, & Der Kiureghian, 2009)

3.4 SUMMARY OF THE PERFORMANCE-BASED EARTHQUAKE ENGINEERING FRAMEWORK

This chapter introduces a fully probabilistic performance-based earthquake engineering evaluation framework and a practical implementation of that framework.

Recognizing that a major obstacle in implementing the performance-based earthquake engineering is the need to conduct numerous dynamic analyses to obtain realizations of response of the structure to likely ground motions occurring on a given site. A method of generating such response realization using a limited number of dynamic analyses is introduced. This method requires a small number of dynamic analyses to generate a database for deriving the correlation among the principal engineering demand parameter needed to evaluate the performance of the building. Once such database is populated, a statistical procedure is used to generate additional vectors of engineering demand parameter with the property that they have the same correlation as the EDPs computed directly by dynamic analysis of the building.

This computationally inexpensive procedure enables a Monte-Carlo type implementation of the PBEE framework (Yang T. , Moehle, Stojadinovic, & Der Kiureghian, 2009). The procedure for the implementation is outlined. It starts with a systematic data collection to describe the seismic environment and the vulnerability of the structure. The seismic environment is described in a seismic hazard analysis. The vulnerability of the structure is described using the fragility of the structural and non-structural components and the associated engineering demand parameters (EDPs), as well as the quantities and repair methods with the associated repair costs of the structural and non-structural components. The seismic response is obtained by conducting a limited number of nonlinear dynamic analysis on a finite element model of the structure. This model generates a database for finding the statistical correlation of the EDPs to the applied ground motion. Once the correlation is defined, a Monte-Carlo technique is used to generate numerous realizations of the seismic response of the building and damage to structural and non-structural components in order to compute the statistics of the total repair cost. Such data are used to express the performance of the structure in terms of total repair cost.

This procedure has been implemented in a computer program called Opensees Navigator to process the computation. An example of using the procedure to evaluate the seismic performance for before and after toggle brace upgrade of the SAC joint venture building is

36

presented in the next chapter. This example illustrates how the PBEE framework can be used to rationalize the selection of a structural system for a new building

CHAPTER 4: PERFORMANCE-BASED EVALUATION OF A TOGGLE BRACE FRAME UPGRADE OF A SAC PRE-NORTHRIDGE DESIGNED MOMENT FRAME

In order to assess the performance of upgrading an existing moment frame design, a prototype of nine-story, five bays by five bays, office building without basement level was selected for this study. Pre-Northridge design of this prototype was assessed subjected to the selected ground motions. This nine-story office building was originally designed as part of the SAC Steel Research Program and was upgraded by addition of toggle brace. In this study, the system performance was assessed using the performance-based earthquake engineering (PBEE) framework presented in the previous chapter. For comparison purpose, both models (before and after the toggle brace upgrade) were evaluated using the same PBEE methodology. This comparison objective was to improve the knowledge base on the seismic behaviour of toggle brace when it is employed to upgrade an existing moment frame.

4.1 DESCRIPTION OF THE BUILDING MODELS

The model selected for this study is a nine-story pre-Northridge design originally designed as part of the SAC Steel Research Program (explained in more detail in Gupta and Krawinkler 1999) Detail descriptions in terms of building dimension and member sizes of this design could be found in the later sections.

In the nine-story pre-Northridge design, one of the exterior bays has only one moment resisting connection to avoid bi-axial bending in the corner column. The pre-Northridge design was based on design practices prevalent before the Northridge earthquake, without the consideration of FEMA 267 (1995) document. This design has standard beam-to-column welded connection details. Fully-restrained steel moment connections were designed following the AISC Manual of Steel Construction. The design yield strength of the beams is 36 ksi and of the columns is 50 ksi.

For the nine-story pre-Northridge design, it has a fixed bay width of 30 feet (9 meter), a first floor height of 18 feet (5.5 meter) and a floor height of 13 feet (4 meter). For the second

38

model, everything in the first model remains the same, except for the addition of toggle brace in one bay of the structure on each level. Since the original SAC frame were designed based on the 1994 Uniform Building Code (UBC 1994), for comparison purposes the same loading were used for both models.

The building models are assumed to be located in downtown Los Angeles, California for the selection of ground motions.

4.1.1 BUILDING DIMENSION AND MEMBER SIZES

As can be seen on Figure 10, the lateral load resisting system is located at the perimeter of the building. Summary of the member sizes of the perimeter moment frames are shown in **Error! Reference source not found.** and Figure 11 Summary of the pre-Northridge moment frame member sizes respectively.
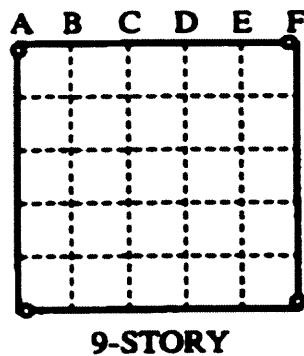
Figure 10 Nine-story pre-Northridge design building plan

Pre-Northridge
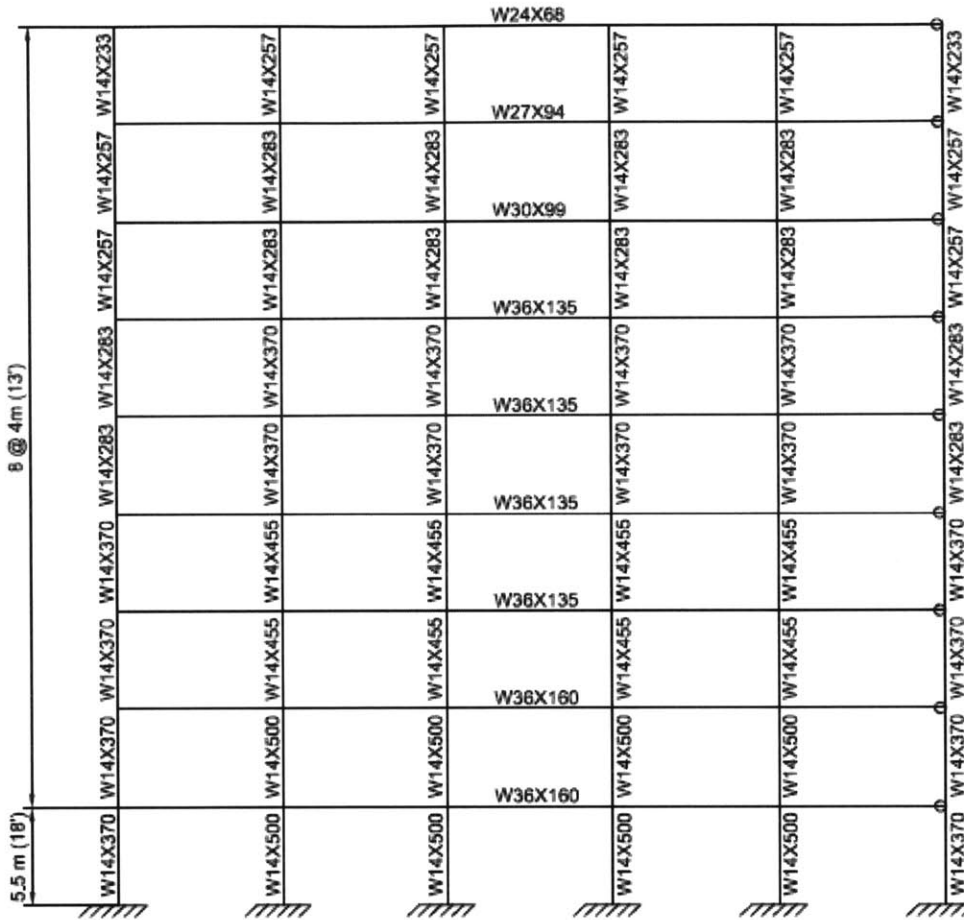
Figure 11 Summary of the pre-Northridge moment frame member sizes

4.1.2 GRAVITY LOAD AND SEISMIC WEIGHT

Since the original SAC frames were designed based on UBC 1994, for comparison purpose the same loading were used for the toggle brace upgrade. The gravity loads were given in the following, and seismic weights are shown on Table 3 (where the values are for one seismic frame), original design parameters were shown in Table 4.

- Floor dead load for weight calculations: 96 psf
- Floor dead load for mass calculations: 86 psf
- Roof dead load excluding penthouse: 83 psf
- Penthouse dead load: 116 psf
- Reduced live load per floor and for roof: 20 psf

40

Table 3 Seismic weights

Floor Level	Weight (kips-sec^2/ft)
Roof	73.1
Floor 3 to Floor 9	67.86
Floor 2	69.04

Table 4 Original design parameters

Parameter	Value
Occupancy Category	Standard
Soil Profile Type	S_D
Importance Factor	1.0
Rw	12
Maximum Drift Ratio	2%

4.1.3 SELECTION OF PERFORMANCE GROUPS

Following the PBEE methodology in the previous chapter, major structural and non-structural components of the building were identified and separated into different performance groups. Each performance group consists of one or more components whose performance is affected in a similar manner by a particular engineering demand parameter. For example, one performance group might comprise all similar non-structural components whose performance is sensitive to the fourth floor inter-story drift, such as glass panels, claddings, and vertical pipelines. For our nine-story pre-Northridge building, major components of the building were divided into 46 performance groups, as shown in Table 5. Some are sensitive to displacement while others are sensitive to acceleration.

Table 5 Summary of performance groups

Name	Location	EDP	Components	Fragilities			
					>= DS2	>= DS3	>= DS4
SH12	between levels 1 and 2	du1		Median EDP	1.7	1.7	2.5
				Beta	0.4	0.4	0.4
SH23	between levels 2 and 3	du2		Median EDP	1.7	1.7	2.5
				Beta	0.4	0.4	0.4
SH34	between levels 3 and 4	du3		Median EDP	1.7	1.7	2.5
				Beta	0.4	0.4	0.4
SH45	between levels 4 and 5	du4	**Structural lateral:** lateral load resisting system; damage oriented fragility (direct loss calculations)	Median EDP	1.7	1.7	2.5
				Beta	0.4	0.4	0.4
SH56	between levels 5 and 6	du5		Median EDP	1.7	1.7	2.5
				Beta	0.4	0.4	0.4
SH67	between levels 6 and 7	du6		Median EDP	1.7	1.7	2.5
				Beta	0.4	0.4	0.4
SH78	between levels 7 and 8	du7		Median EDP	1.7	1.7	2.5
				Beta	0.4	0.4	0.4
SH89	between levels 8 and 9	du8		Median EDP	1.7	1.7	2.5
				Beta	0.4	0.4	0.4
SH9R	between levels 9 and R	du9		Median EDP	1.7	1.7	2.5
				Beta	0.4	0.4	0.4
EXTD1 2	between levels 1 and 2	du1		Median EDP	2.8	3.1	
				Beta	0.097	0.12	
EXTD2 3	between levels 2 and 3	du2	**Exterior enclosure:** panels, glass, etc.	Median EDP	2.8	3.1	
				Beta	0.097	0.12	
EXTD3 4	between levels 3 and 4	du3		Median EDP	2.8	3.1	
				Beta	0.097	0.12	

42

EXTD4 5	between levels 4 and 5	du4		Median EDP	2.8	3.1	
				Beta	0.097	0.12	
EXTD5 6	between levels 5 and 6	du5		Median EDP	2.8	3.1	
				Beta	0.097	0.12	
EXTD6 7	between levels 6 and 7	du6		Median EDP	2.8	3.1	
				Beta	0.097	0.12	
EXTD7 8	between levels 7 and 8	du7		Median EDP	2.8	3.1	
				Beta	0.097	0.12	
EXTD8 9	between levels 8 and 9	du8		Median EDP	2.8	3.1	
				Beta	0.097	0.12	
EXTD9 R	between levels 9 and R	du9		Median EDP	2.8	3.1	
				Beta	0.097	0.12	
INTD1 2	between levels 1 and 2	du1		Median EDP	0.39	0.85	
				Beta	0.17	0.23	
INTD2 3	between levels 2 and 3	du2		Median EDP	0.39	0.85	
				Beta	0.17	0.23	
INTD3 4	between levels 3 and 4	du3		Median EDP	0.39	0.85	
				Beta	0.17	0.23	
INTD4 5	between levels 4 and 5	du4	**Interior nonstructural drift sensitive:** partitions, doors, glazing, etc	Median EDP	0.39	0.85	
				Beta	0.17	0.23	
INTD5 6	between levels 5 and 6	du5		Median EDP	0.39	0.85	
				Beta	0.17	0.23	
INTD6 7	between levels 6 and 7	du6		Median EDP	0.39	0.85	
				Beta	0.17	0.23	
INTD7 8	between levels 7 and 8	du7		Median EDP	0.39	0.85	
				Beta	0.17	0.23	
INTD8 9	between levels 8 and 9	du8		Median EDP	0.39	0.85	
				Beta	0.17	0.23	

INTD9R	between levels 9 and R	du9		Median EDP	0.39	0.85	
				Beta	0.17	0.23	
INTA2	below level 2	a2		Median EDP	1	1.5	2
				Beta	0.15	0.2	0.2
INTA3	below level 3	a3		Median EDP	1	1.5	2
				Beta	0.15	0.2	0.2
INTA4	below level 4	a4		Median EDP	1	1.5	2
				Beta	0.15	0.2	0.2
INTA5	below level 5	a5		Median EDP	1	1.5	2
			Interior nonstructural acceleration sensitive: ceilings, lights, sprinkler heads, etc	Beta	0.15	0.2	0.2
INTA6	below level 6	a6		Median EDP	1	1.5	2
				Beta	0.15	0.2	0.2
INTA7	below level 7	a7		Median EDP	1	1.5	2
				Beta	0.15	0.2	0.2
INTA8	below level 8	a8		Median EDP	1	1.5	2
				Beta	0.15	0.2	0.2
INTA9	below level 9	a9		Median EDP	1	1.5	2
				Beta	0.15	0.2	0.2
INTAR	below level R	aR		Median EDP	1	1.5	2
				Beta	0.15	0.2	0.2
CONT1	at level 1	ag		Median EDP	0.3	0.7	3.5
				Beta	0.2	0.22	0.25
CONT2	at level 2	a2	**Contents**: General office on first and second floor, computer center on third	Median EDP	0.3	0.7	3.5
				Beta	0.2	0.22	0.25
CONT3	at level 3	a3		Median EDP	0.3	0.7	3.5
				Beta	0.2	0.22	0.25
CONT4	at level 4	a4		Median EDP	0.3	0.7	3.5
				Beta	0.2	0.22	0.25

44

CONT5	at level 5	a5		Median EDP	0.3	0.7	3.5
				Beta	0.2	0.22	0.25
CONT6	at level 6	a6		Median EDP	0.3	0.7	3.5
				Beta	0.2	0.22	0.25
CONT7	at level 7	a7		Median EDP	0.3	0.7	3.5
				Beta	0.2	0.22	0.25
CONT8	at level 8	a8		Median EDP	0.3	0.7	3.5
				Beta	0.2	0.22	0.25
CONT9	at level 9	a9		Median EDP	0.3	0.7	3.5
				Beta	0.2	0.22	0.25
EQUIP R	at level R	aR	**Equipment on roof**	Median EDP	1	2	
				Beta	0.15	0.2	

Since the severity of the damage will determine the repair action, multiple damage states are defined for each performance group. For each component damage state, a fragility relation defines the probability of component damage being equal to or greater than the threshold damage given the value of engineering demand parameter associated with the component.   Figure 12 to Figure 17 show the fragility curves used to identify the damage state of each performance group. Because the fragility functions for each floor are the same (assuming identical occupancy category), it is sufficient to only show one fragility curve per performance group. The fragility models were obtained through FEMA P-58-1, and an objective of this study was to demonstrate their implementation.
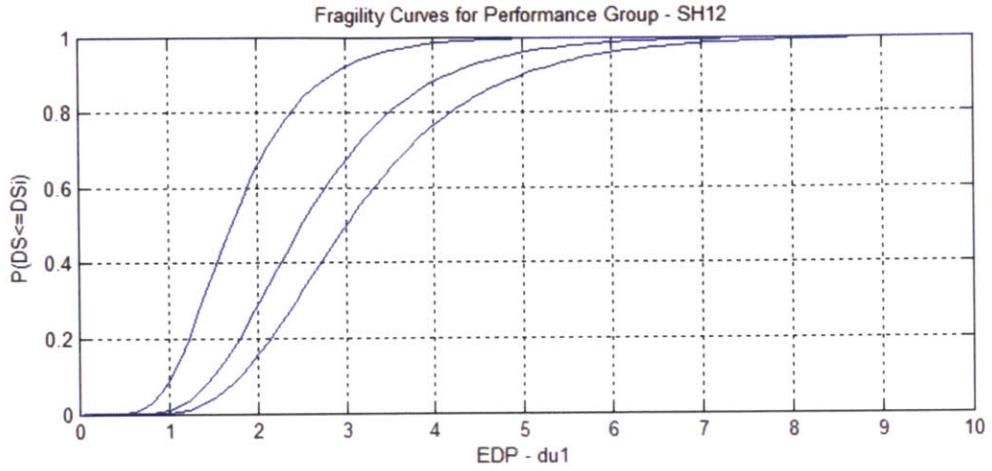
Figure 12 Fragility curves for performance group - SHs
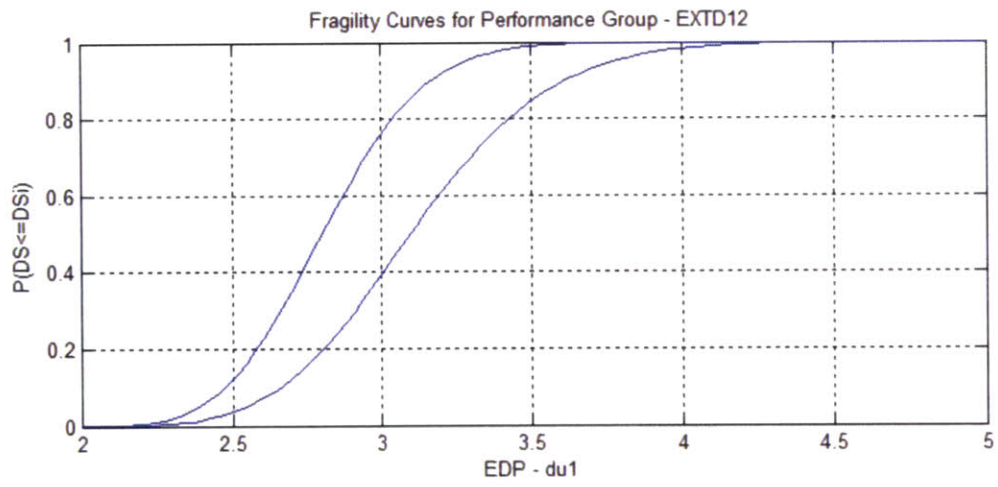
Figure 13 Fragility curves for performance group - EXTDs
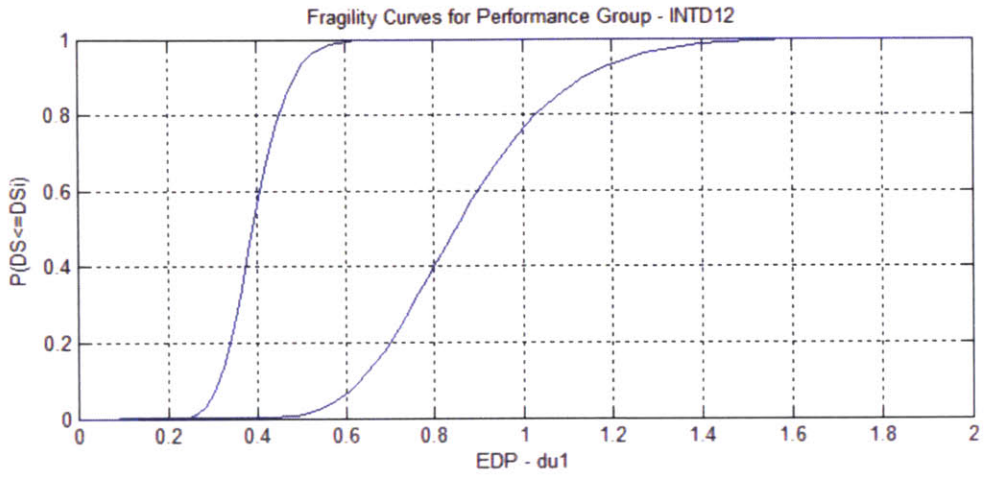
Figure 14 Fragility curves for performance group - INTDs
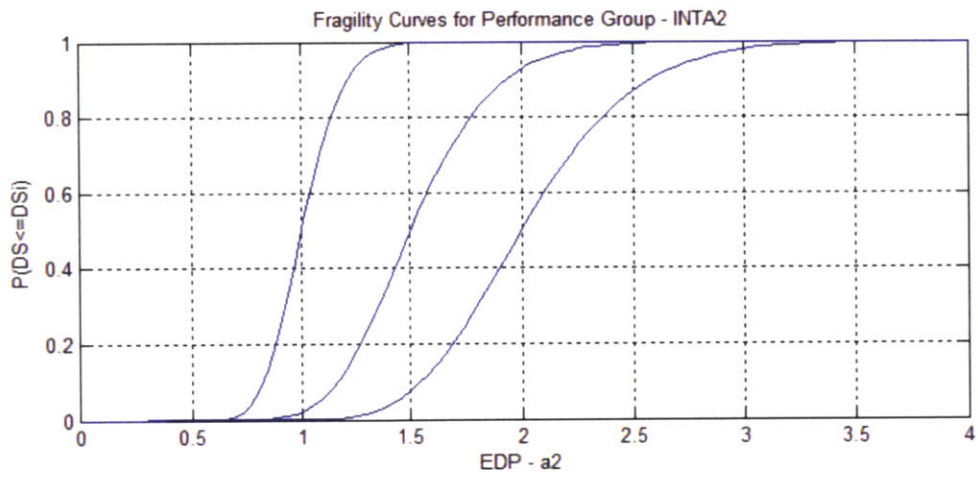
Figure 15 Fragility curves for performance group - INTAs
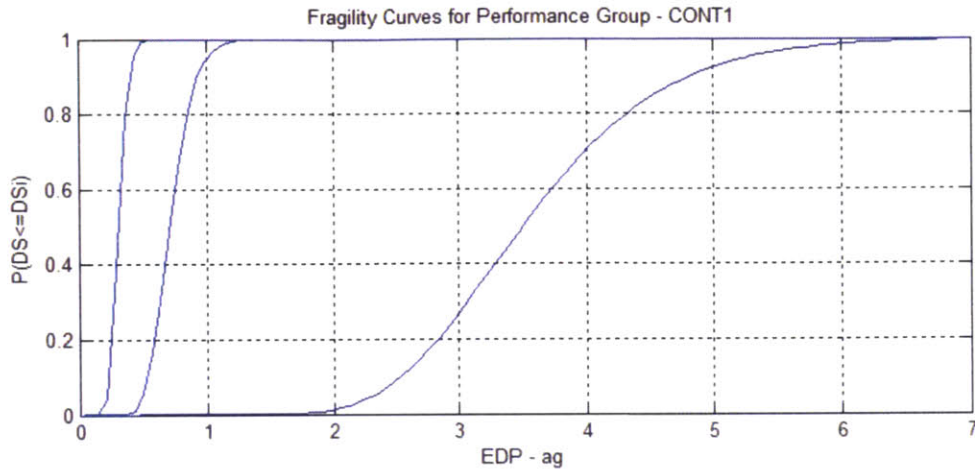
Figure 16 Fragility curves for performance group - CONTs
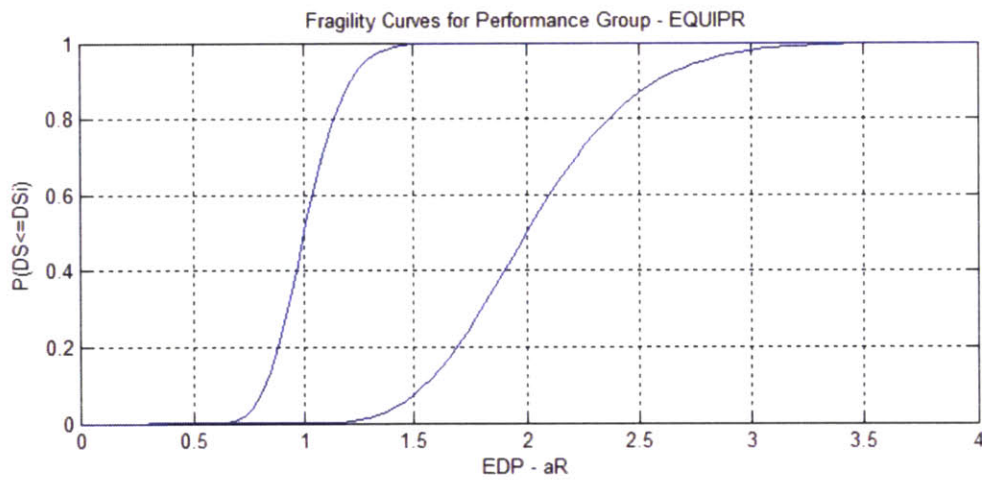
Figure 17 Fragility curves for performance group - EQUIPR

Based on repair actions, repair quantities for each item in any performance groups are shown from Table 6 to

Table 9. These values are obtained from FEMA P-58-1 (Mieler, Stojadinovic, Budnitz, Mahin, & Comoerio, 2013). Following the methodology outlined in the previous chapter, cost model can be created for the performance assessment of the structural models.

Table 6 Repair quantities for PG37-PG45

Repair Items	PG37 - PG45 CONTs			
	DS1	DS2	DS3	DS4
Office papers and books	0	0	9896	9896
Office equipment	0	4948	9896	9896
Loose furniture, file, drawers	0	9896	19792	19792
Water damage	0	0	4948	9896
Conventional office	0	0	0	19792

Table 7 Repair quantities for PG1 - PG9

Repair Items	PG1 - PG9 SHs					
	DS1	DS2	DS3	DS4	DS5	DS6
Post-Northridge MRF Connection DS1	0	10	0	0	0	0
Post-Northridge MRF Connection DS2	0	0	10	0	0	0
Post-Northridge MRF Connection DS3	0	0	0	10	0	0
Post-Northridge MRF Connection DS4	0	0	0	0	10	0
Post-Northridge MRF Connection DS5	0	0	0	0	0	10
Finish protection	0	16667	16667	16667	n/a	n/a
Ceiling system removal	0	8333	8333	13889	n/a	n/a
Drywall assembly removal	0	2222	2222	16667	n/a	n/a
Miscellaneous MEP	0	6	11	17	n/a	n/a
Remove exterior skin	0	0	0	8333	n/a	n/a
Welding protection	0	4167	4167	4167	n/a	n/a
Shore beams below remove	0	0	0	33	n/a	n/a
Cut floor slab at damaged conn	0	194	417	4444	n/a	n/a
Carbon arc out weld	0	111	139	139	n/a	n/a
Remove portion of damaged beam col	0	0	278	278	n/a	n/a
Replace weld from above	0	111	111	111	n/a	n/a

Remove replace connection	0	0	0	5556	n/a	n/a
Replace slab	0	194	194	4444	n/a	n/a
Miscellaneous MEP and cleanup	0	6	11	17	n/a	n/a
Wall framing(studs drywall tape paint)	0	2222	2222	16667	n/a	n/a
Replace exterior skin(from salvage)	0	0	0	15556	n/a	n/a
Ceiling system	0	8333	8333	13889	n/a	n/a

Table 8 Repair quantities for PG19 – PG27

Repair Items	PG19 – PG27 INTDs		
	DS1	DS2	DS3
Remove furniture	0	4948	9896
Carpet and rubber base removal	0	0	9896
Drywall construction removal	0	0	9896
Door and frame removal	0	8	8
Interior glazing removal	0	99	99
Ceiling_system_removal2	0	0	4948
MEP removal	0	0	990
Remove casework	0	0	198
Drywall construction paint	0	0	9896
Doors and frames	0	8	25
Interior glazing	0	99	396
Carpet and rubber base	0	0	9896
Patch and paint interior partitions	0	4948	4948
Replace ceiling tiles	0	0	0
Replace ceiling system	0	0	4948
MEP replacement	0	0	990
Replace casework	0	0	198

50

Table 9 Repair quantities for PG10 –PG18

Repair Items	PG10 – PG18 EXTDs		
	DS1	DS2	DS3
Remove furniture	0	5904	5904
Remove damaged windows	0	3345	3345
Remove damage precast panels (demo)	0	0	8265
Miscellaneous access	0	8265	8265
Install new windows	0	3345	3345
Provide new precast concrete panels	0	0	8265
Patch and paint exterior panels	0	4920	4920
Miscellaneous put back	0	8265	8265
Site clean up	0	5904	5904

The unit cost of repair item generally reduces as the increase of the repair quantities for repair items, the unit cost function for each repair item is generally tri-linear. An example of such unit cost function is shown in Figure 18. Uncertainties of the unit repair cost can be accounted for in the cost model by treating the repair cost as a normally distributed random variable with second moment information, for simplicities of calculation, such uncertainties were not assigned for this study. The values for different unit cost functions are summarized in Table 11.
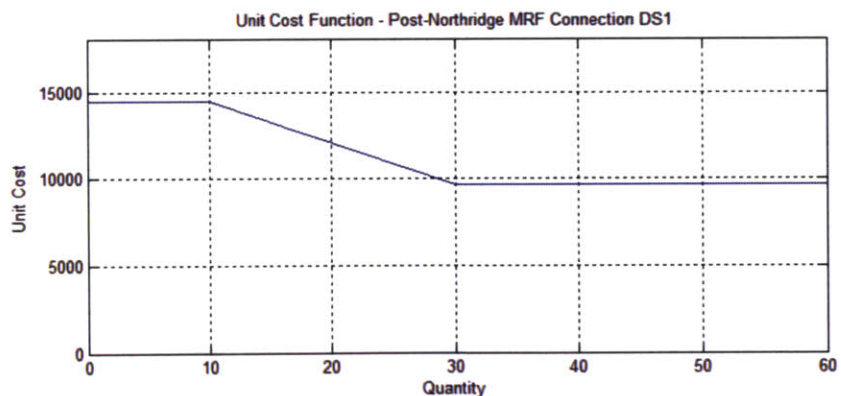
Figure 18 An example of unit cost function

Table 10 Summary of values for unit cost functions

Item Name	Min.Qty.	Max.Qty.	Max. cost (Median)	Min. cost (Median)	Cost uncertainty
Office papers books	1000	10000	0.1	0.06	0
Office equipment	1000	10000	0.06	0.04	0
Loose furniture file drawers	1000	10000	0.05	0.03	0
Water damage	1000	20000	0.15	0.1	0
Conventional office	10000	50000	25	21	0
Repair in place	1	2	10000	10000	0
Remove and replace	1	2	200000	200000	0
Finish protection	1000	40000	0.3	0.15	0
Ceiling_system_removal1	1000	10000	2	1.25	0
Drywall assembly removal	1000	20000	2.5	1.5	0
Miscellaneous MEP	6	24	200	150	0
Remove exterior skin	3000	10000	30	25	0
Welding protection	1000	10000	1.5	1	0
Shore beams below remove	6	24	2100	1600	0
Cut floor slab at damaged conn	10	100	200	150	0
Carbon arc out weld	100	1000	15	10	0
Remove portion of damaged beam col	100	2000	80	50	0
Replace weld from above	100	1000	50	40	0
Remove replace connection	2000	20000	6	5	0
Replace slab	100	1000	20	16	0
Miscellaneous MEP and cleanup	6	24	300	200	0
Wall framing (studs drywall tape paint)	100	1000	12	8	0
Replace exterior skin (from salvage)	1000	10000	35	30	0
Ceiling system	100	60000	8	5	0
Remove furniture	100	1000	2	1.25	0

Carpet and rubber base removal	1000	20000	1.5	1	0
Drywall construction removal	200	20000	2.5	1.5	0
Door and frame removal	12	48	40	25	0
Interior glazing removal	500	5000	2.5	2	0
Ceiling_system_removal2	1000	20000	2	1.25	0
MEP removal	100	10000	40	15	0
Remove casework	100	1000	20	15	0
Drywall construction paint	500	25000	12	8	0
Doors and frames	12	48	600	400	0
Interior glazing	100	15000	45	30	0
Carpet and rubber base	500	30000	6	4	0
Patch and paint interior partitions	1000	10000	2.5	2	0
Replace ceiling tiles	1000	20000	2	1.5	0
Replace ceiling system	1000	20000	3	2.5	0
MEP replacement	100	1000	80	60	0
Replace casework	100	1000	70	50	0
Erect scaffolding	1000	10000	2.5	2	0
Remove damaged windows	100	1000	20	15	0
Remove damage precast panels (demo)	3000	10000	12	8	0
Miscellaneous access	100	1000	20	15	0
Install new windows	100	1000	80	70	0
Provide new precast concrete panels	1000	10000	80	65	0
Patch and paint exterior panels	500	5000	4.5	3.5	0
Miscellaneous put back	100	1000	10	7	0
Site clean up	1000	10000	1.5	0.75	0

4.2 DESCRIPTION OF THE ANALYTICAL MODEL

Structural element models, representing SAC pre-Northridge moment frame before and after the upgrade of toggle brace, were built in SAP2000. The 2-D model shows the building

53

configuration oriented in the North-South direction for simplicity purpose. The frame only represents half of the structure. Beams and columns consist of elastic regions, plastic hinges as a zero length element, and rigid end zones at each end. For beams-to-column connections, the moment-rotation relationship was modelled with a tri-linear backbone curve including the strength loss and cyclic degradation. The related parameters for connections were obtained from experimental data calibration. In order to account for the possible yielding in the panel zones, panel zones were modelled using auto connection panel zone in SAP 2000. For column elements, an additional moment-axial interaction curve was used in order to calculate structural response. A lumped P-delta column was used to include the P-delta effects caused by the vertical loads tributary to the interior frames, which was transferred to the moment resisting frame through the rigid slab. Seismic mass was calculated based on tributary area and lumped at the central nodes at each floor level. Seismic loads were applied at lateral direction, which was parallel to the structure orientation. Rayleigh damping ratio of 2% was assigned in the nonlinear dynamic modelling of the building. Table 11 shows the first three mode periods of the buildings

Table 11 Periods of the first three modes for prototype buildings

Modes	Periods (Seconds)
1st	2.357
2nd	0.883
3rd	0.510

4.2.1 BEHAVIOUR AND MODELLING OF PRE-NORTHRIDGE CONNECTIONS

The pre-Northridge design was based on design practices prevalent before the Northridge earthquake (UBC 1994), without the consideration of FEMA 267 (1995) document. This design has standard beam-to-column welded connection details. Fully-restrained steel moment connections were designed following the AISC Manual of Steel Construction. The design yield strength of the beams is 36 ksi and of the columns is 50 ksi. Experimental data was obtained for a typical fully restrained pre-Northridge connection and adjustable parameters in SAP2000 were

54

calibrated to model this connection. The experimental (obtained from SAC database) and calibrated cyclic degradation curve for the plastic hinge is shown in Figure 19 respectively.
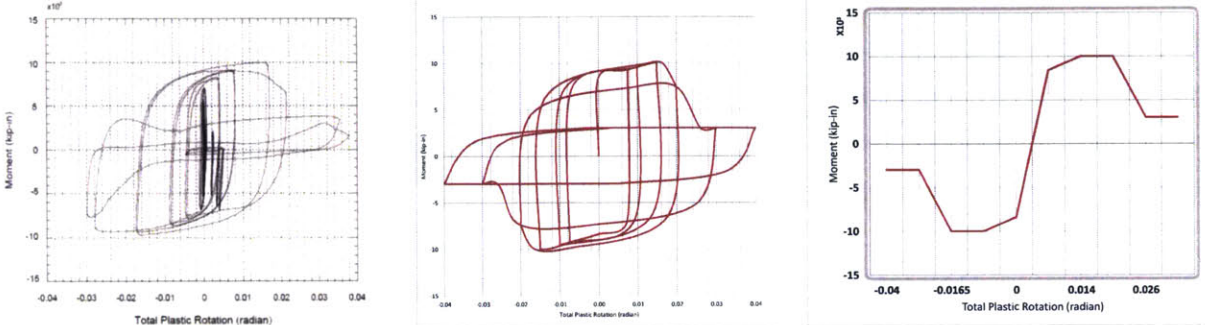

Figure 19 Experimental and model moment-rotation relation for pre-Northridge connection

4.3 SELECTION OF THE GROUND MOTIONS

Sets of ground motions representative of different hazard levels have been assembled for the location of downtown Los Angeles as part of the SAC steel research project (SAC Joint Venture, 2000). The sets consist of recorded and simulated ground motions and represent return periods of 72 years (50% probability of being exceeded in 50 years; referred to as the 50/50 sets), 475 years (10% probability of being exceeded in 50 years; referred to as the 10/50 sets), and 2475 years (2% probability of being exceeded in 50 years; referred to as the 2/50 sets). Each set of ground motions consists of 20 time histories; 10 ground motions each with 2 orthogonal components. The individual components of all the records have been rotated to 45 degrees with respect to the fault in order to minimize directivity effects.

The ground motions are scaled such that, on average, their spectral values match with a least square error fit to the United States Geological Survey's (USGS) mapped values at 0.3, 1.0, and 2.0 seconds, and an additional predicted value at 4.0 seconds (Somerville et al., 1997). The weights ascribed to the four period points are 0.1 at the 0.3 second period point and 0.3 for the other three period points. The target spectra provided by USGS are for the SB/SC soil type boundaries, which have been modified to be representative for soil type SD (stiff soil – measure shear wave velocity between 6000 to 1200 ft/sec). Details concerning the modification factors used to transform the target response spectra to be representative of soil type SD, and the scaling

55

factors used for the individual ground motions are given in Somerville et al. (1997). The target response spectra values for soil type SD are reproduced in Table 12.

Table 13 to Table 15 provide basic information for the individual earthquake records constituting the different sets of ground motions for Los Angeles. The duration of the ground motion records given in Table 13 to Table 15 signifies the total length of the time history. The entire length of the time history is used for analysis, i.e., the time history is not curtailed to reflect only the strong motion duration of the record.

The target spectra given by USGS and the spectra accelerations for the different sets of earthquake after scaling are shown in Table 12 (for 5% damping). An idea of the relative seismic hazard in the different regions can be obtained from these numbers.

Table 12 Target response spectra values for soil type S_D for 5% damping level (from Somerville et al., 1997)

Location	Hazard Level	Period			
		0.3	1.0	2.0	4.0
Los Angeles	50/50	0.514	0.288	0.149	0.069
	10/50	1.070	0.680	0.330	0.123
	2/50	1.610	1.190	0.540	0.190

Table 13 Basic characteristics of Los Angeles ground motion records

50/50 Set of Records (72yrs return period)							
Designation	**Record**	**Earthquake**	**Distance**	**Scale**	**Number**	**Duration**	**PGA**
		Magnitude	**(km)**	**Factor**	**of Points**	**(sec)**	**(cm/sec²)**
LA41	Coyote Lake, 1979	5.7	8.8	2.28	2686	39.38	578.34
LA42	Coyote Lake, 1979	5.7	8.8	2.28	2686	39.38	326.81
LA43	Imperial Valley, 1979	6.5	1.2	0.4	3909	39.08	140.67
LA44	Imperial Valley, 1979	6.5	1.2	0.4	3909	39.08	109.45
LA45	Kern, 1952	7.7	107	2.92	3931	78.6	141.49
LA46	Kern, 1952	7.7	107	2.92	3931	78.6	156.02
LA47	Landers, 1992	7.3	64	2.63	4000	79.98	331.22
LA48	Landers, 1992	7.3	64	2.63	4000	79.98	301.74
LA49	Morgan Hill, 1984	6.2	15	2.35	3000	59.98	312.41
LA50	Morgan Hill, 1984	6.2	15	2.35	3000	59.98	535.88
LA51	Parkfield, 1966, Cholame 5W	6.1	3.7	1.81	2197	43.92	765.65
LA52	Parkfield, 1966, Cholame 5W	6.1	3.7	1.81	2197	43.92	619.36
LA53	Parkfield, 1966, Cholame 8W	6.1	8	2.92	1308	26.14	680.01
LA54	Parkfield, 1966, Cholame 8W	6.1	8	2.92	1308	26.14	775.05
LA55	North Palm Springs, 1986	6	9.6	2.75	3000	59.98	507.58
LA56	North Palm Springs, 1986	6	9.6	2.75	3000	59.98	371.66
LA57	San Fernando, 1971	6.5	1	1.3	3974	79.46	248.14
LA58	San Fernando, 1971	6.5	1	1.3	3974	79.46	226.54
LA59	Whittier, 1987	6	17	3.62	2000	39.98	753.7
LA60	Whittier, 1987	6	17	3.62	2000	39.98	469.07

Table 14 (cont'd) Basic characteristics of Los Angeles ground motion records

SAC Name	Record	Earthquake Magnitude	Distance (km)	Scale Factor	Number of Points	Duration (sec)	PGA (cm/sec²)
		10/50 Set of Records (475yrs return period)					
LA01	Imperial Valley, 1940, El Centro	6.9	10	2.01	2674	39.38	452.03
LA02	Imperial Valley, 1940, El Centro	6.9	10	2.01	2674	39.38	662.88
LA03	Imperial Valley, 1979, Array #05	6.5	4.1	1.01	3939	39.38	386.04
LA04	Imperial Valley, 1979, Array #05	6.5	4.1	1.01	3939	39.38	478.65
LA05	Imperial Valley, 1979, Array #06	6.5	1.2	0.84	3909	39.08	295.69
LA06	Imperial Valley, 1979, Array #06	6.5	1.2	0.84	3909	39.08	230.08
LA07	Landers, 1992, Barstow	7.3	36	3.2	4000	79.98	412.98
LA08	Landers, 1992, Barstow	7.3	36	3.2	4000	79.98	417.49
LA09	Landers, 1992, Yermo	7.3	25	2.17	4000	79.98	509.7
LA10	Landers, 1992, Yermo	7.3	25	2.17	4000	79.98	353.35
LA11	Loma Prieta, 1989, Gilroy	7	12	1.79	2000	39.98	652.49
LA12	Loma Prieta, 1989, Gilroy	7	12	1.79	2000	39.98	950.93
LA13	Northridge, 1994, Newhall	6.7	6.7	1.03	3000	59.98	664.93
LA14	Northridge, 1994, Newhall	6.7	6.7	1.03	3000	59.98	644.49
LA15	Northridge, 1994, Rinaldi RS	6.7	7.5	0.79	2990	14.945	523.3
LA16	Northridge, 1994, Rinaldi RS	6.7	7.5	0.79	2990	14.945	568.58
LA17	Northridge, 1994, Sylmar	6.7	6.4	0.99	3000	59.98	558.43
LA18	Northridge, 1994, Sylmar	6.7	6.4	0.99	3000	59.98	801.44
LA19	North Palm Springs, 1986	6	6.7	2.97	3000	59.98	999.43
LA20	North Palm Springs, 1986	6	6.7	2.97	3000	59.98	967.61

Table 15 (cont'd) Basic characteristics of Los Angeles ground motion records

SAC Name	Record	Earthquake Magnitude	Distance (km)	Scale Factor	Number of Points	Duration (sec)	PGA (cm/sec^2)
	2/50 Set of Records (2475yrs return period)						
LA21	1995 Kobe	6.9	3.4	1.15	3000	59.98	1258
LA22	1995 Kobe	6.9	3.4	1.15	3000	59.98	902.75
LA23	1989 Loma Prieta	7	3.5	0.82	2500	24.99	409.95
LA24	1989 Loma Prieta	7	3.5	0.82	2500	24.99	463.76
LA25	1994 Northridge	6.7	7.5	1.29	2990	14.945	851.62
LA26	1994 Northridge	6.7	7.5	1.29	2990	14.945	925.29
LA27	1994 Northridge	6.7	6.4	1.61	3000	59.98	908.7
LA28	1994 Northridge	6.7	6.4	1.61	3000	59.98	1304.1
LA29	1974 Tabas	7.4	1.2	1.08	2500	49.98	793.45
LA30	1974 Tabas	7.4	1.2	1.08	2500	49.98	972.58
LA31	Elysian Park (simulated)	7.1	17.5	1.43	3000	29.99	1271.2
LA32	Elysian Park (simulated)	7.1	17.5	1.43	3000	29.99	1163.5
LA33	Elysian Park (simulated)	7.1	10.7	0.97	3000	29.99	767.26
LA34	Elysian Park (simulated)	7.1	10.7	0.97	3000	29.99	667.59
LA35	Elysian Park (simulated)	7.1	11.2	1.1	3000	29.99	973.16
LA36	Elysian Park (simulated)	7.1	11.2	1.1	3000	29.99	1079.3
LA37	Palos Verdes (simulated)	7.1	1.5	0.9	3000	59.98	697.84
LA38	Palos Verdes (simulated)	7.1	1.5	0.9	3000	59.98	761.31
LA39	Palos Verdes (simulated)	7.1	1.5	0.88	3000	59.98	490.58
LA40	Palos Verdes (simulated)	7.1	1.5	0.88	3000	59.98	613.28

4.4 RESPONSE QUANTIFICATION

Non-linear dynamic analyses were carried out in SAP2000 to determine the system response of the prototype buildings, 9-story moment frame before and after the toggle brace damper upgrade. Each frame was subjected to 3 different intensity levels of ground motion, each intensity level contained 20 ground motions. Therefore, there were 20 sets of system responses for each frame at each intensity levels. These responses were processed to extract maximum drifts ratios and maximum floor accelerations. The extracted values were created as vectors of Engineering Demand Parameters (EDPs) for cost simulation processes.

To compare the system response among the different hazard levels, the mean peak interstory drift ratios and floor accelerations accompanying their standard deviations were plotted in Figure 20 to Figure 31.

At 50% and 10% probability of exceedance in 50 years hazard level (72 and 475 years return period), the SAC frame upgraded with toggle brace frame performed much better than the original SAC moment frame in terms of maximum drift ratio and maximum floor accelerations (approximately 50% reduction). The variance of maximum drift ratios and maximum accelerations are also smaller than the original SAC moment frame. Both frames experience quite uniform drifts and floor accelerations, this is because most of the frame is still within elastic region.

As the ground motion increases to a 5% probability of exceedance in 50 years hazard level (2475 years return period), the SAC frame upgraded with toggle brace frame experiences much less drifts and floor accelerations while maintaining a uniform profile in terms of drift and acceleration. However, the original SAC moment frame experiences an increase of drifts as the story number decreases. This is because at higher intensity ground motions, the original SAC frame forms multiple hinges at lower levels, this reduces the stiffness at the lower storeys and subsequently result in greater drift ratios.
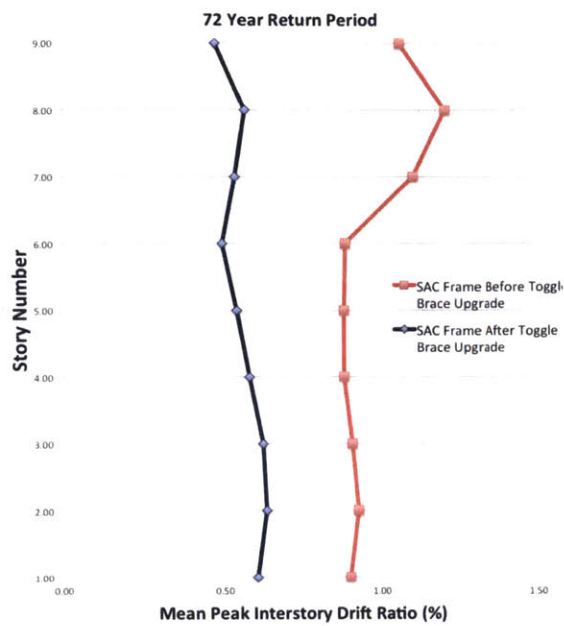
Figure 20 Mean Drift Response Comparison of SAC Frame Before and After Toggle Brace Upgrade Subjected to 72 Year Return Period Ground Motion
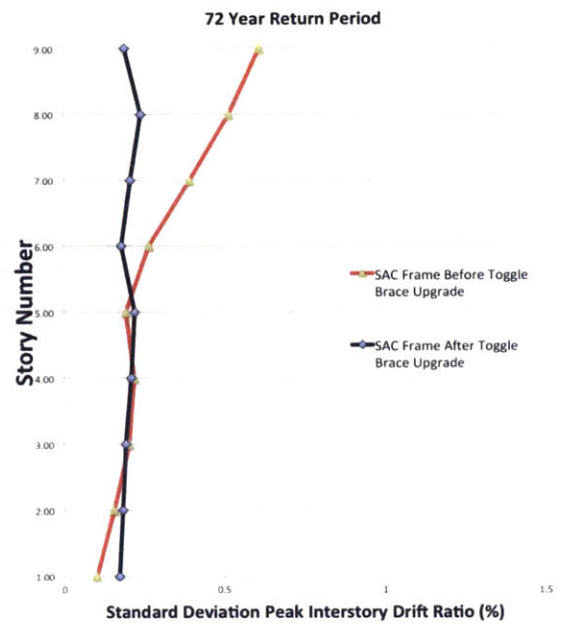

Figure 21 Standard Deviation of Drift Response Comparison of SAC Frame Before and After Toggle Brace Upgrade Subjected to 72 Year Return Period Ground Motion
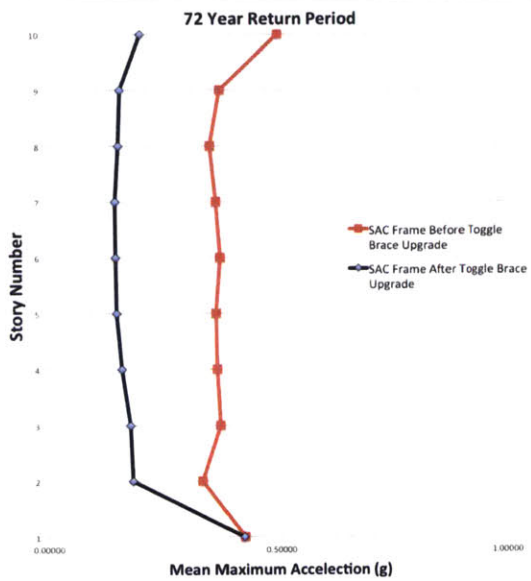

Figure 22 Mean Maximum Acceleration Response Comparison of SAC Frame Before and After Toggle Brace Upgrade Subjected to 72 Year Retun Period Ground Motion
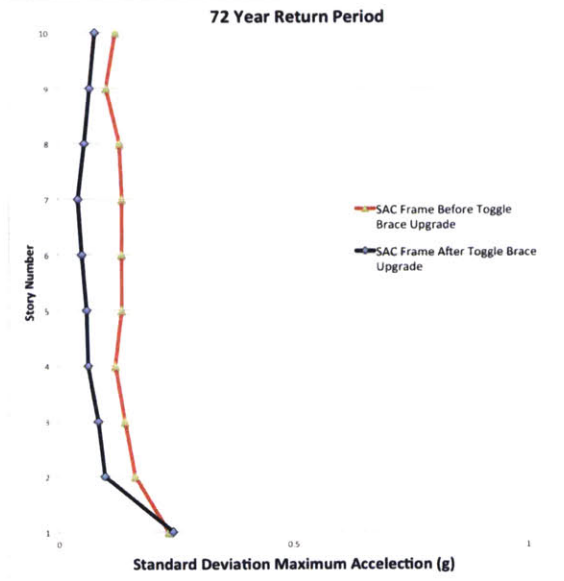

Figure 23 Standard Deviation of Maximum Acceleration Response Comparison of SAC Frame Before and After Toggle Brace Upgrade Subjected to 72 Year Retun Period Ground Motion
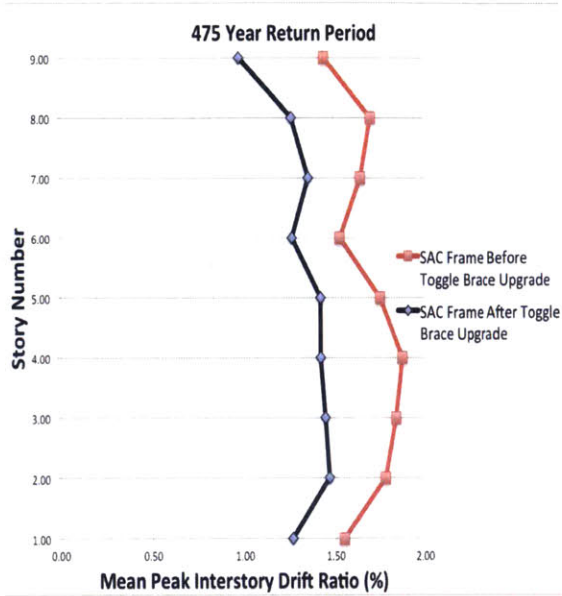
61

Figure 24 Mean Drift Response Comparison of SAC Frame Before and After Toggle Brace Upgrade Subjected to 475 Year Retun Period Ground Motion
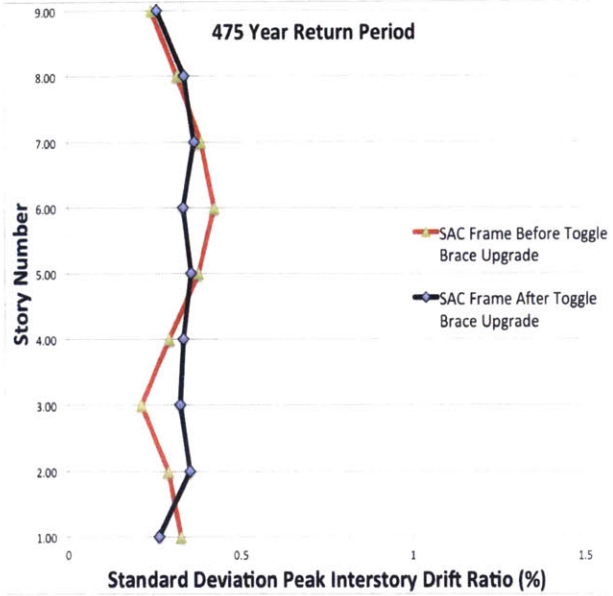

Figure 25 Standard Deviation of Drift Response Comparison of SAC Frame Before and After Toggle Brace Upgrade Subjected to 475 Year Retun Period Ground Motion

Figure 26 Mean Maximum Acceleration Response Comparison of SAC Frame Before and After Toggle Brace Upgrade Subjected to 475 Year Retun Period Ground Motion

Figure 27 Standard Deviation of Maximum Acceleration Response Comparison of SAC Frame Before and After Toggle Brace Upgrade Subjected to 475 Year Retun Period Ground Motion

62
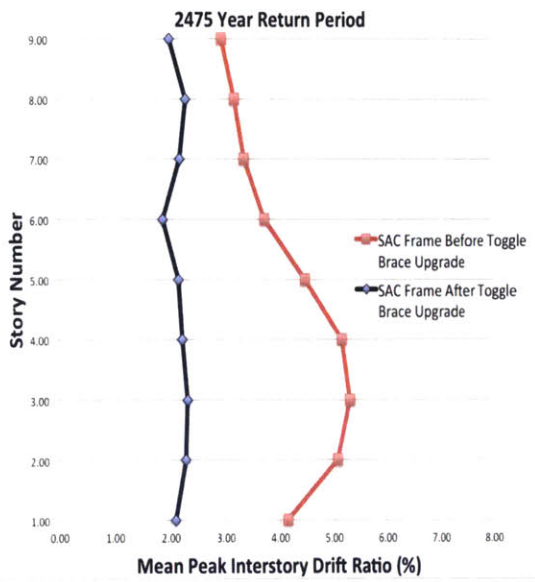
Figure 28 Mean Drift Response Comparison of SAC Frame Before and After Toggle Brace Upgrade Subjected to 2475 Year Retun Period Ground Motion

Figure 29 Standard Deviation of Drift Response Comparison of SAC Frame Before and After Toggle Brace Upgrade Subjected to 2475 Year Retun Period Ground Motion
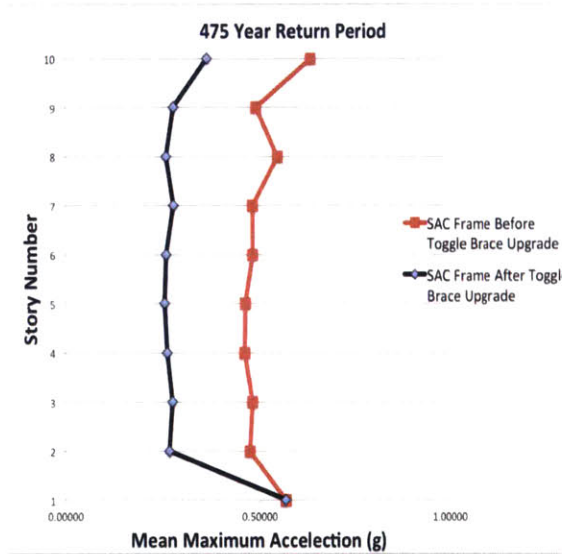

Figure 30 Mean Maximum Acceleration Response Comparison of SAC Frame Before and After Toggle Brace Upgrade Subjected to 475 Year Retun Period Ground Motion
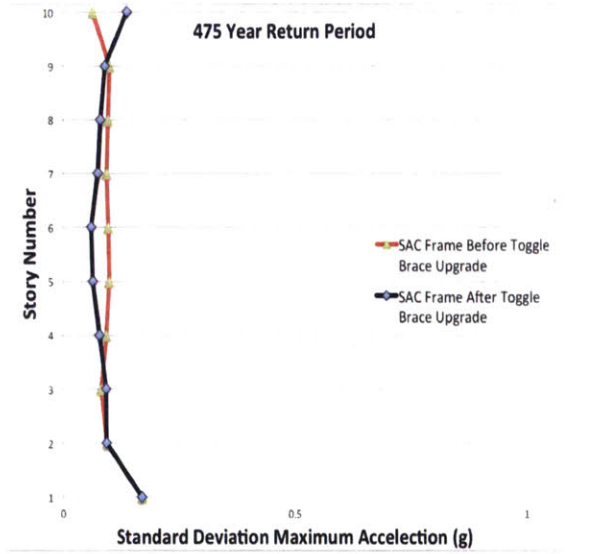

Figure 31 Standard Deviation of Maximum Acceleration Response Comparison of SAC Frame Before and After Toggle Brace Upgrade Subjected to 475 Year Retun Period Ground Motion

63

4.5 COST SIMULATION
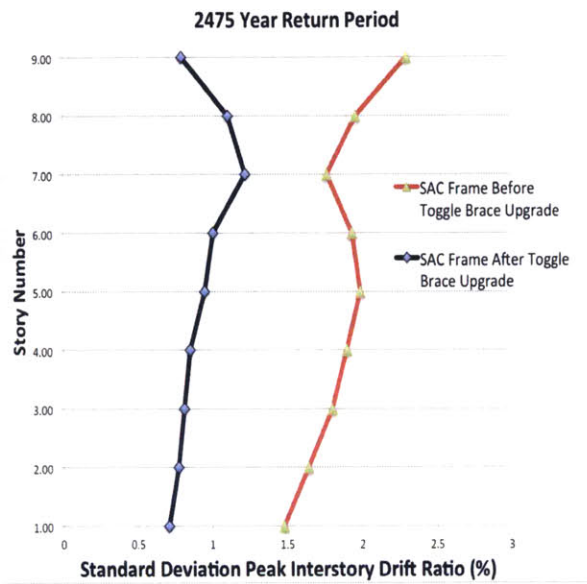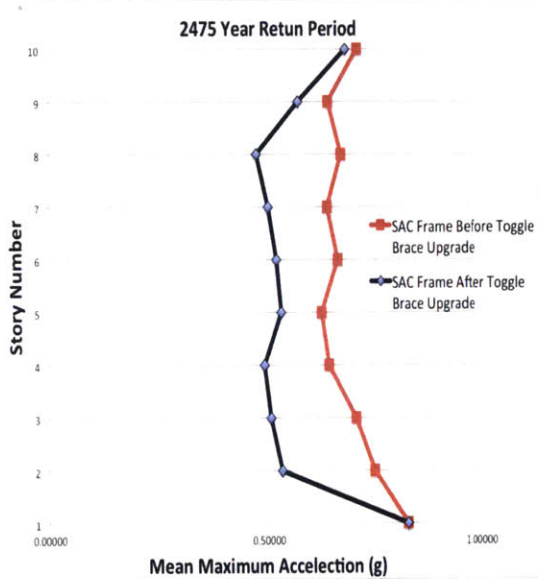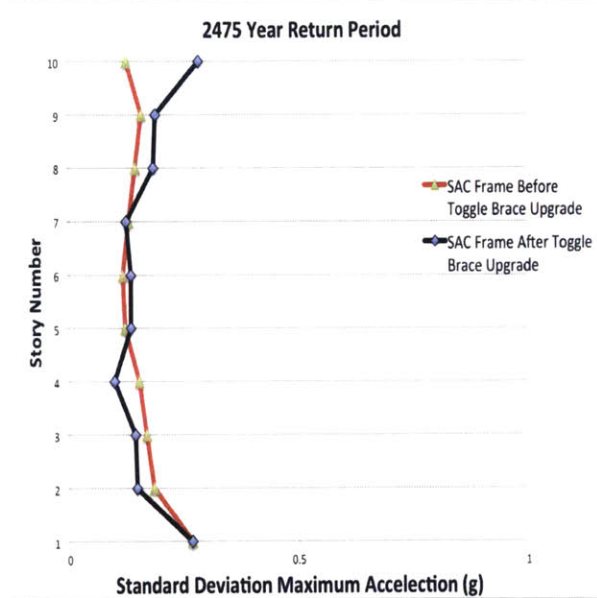
The repair cost simulation was conducted using the PBEE methodology described in the previous chapter and the quantity and cost data presented earlier in this chapter. The discrete cumulative distribution function of the total repair costs for the SAC nine-story moment frame before and after the toggle brace damper upgrade for the three hazard levels considered are shown in Figure 32 to Figure 34, while the log-normal cumulative distribution function of the total repair costs are shown in Figure 35 to Figure 37.

The results of the different probability of exceedance in 50 years hazard level indicate that toggle brace damper upgrade result in significantly lower repair cost. The three different comparisons clearly show that the toggle brace damper upgrade reduces the vulnerability of the original pre-Northridge design under all seismic hazard scenarios. For example, with the 50% probability of exceedance in 50 years hazard level, the probability of probability of total repair cost is less than or equal to $1 million dollars is 12% for the original SAC frame and 52% for the toggle brace upgraded frame.

Figure 32 Discrete CDF of the repair cost distribution for 72 years return period intensity level

Figure 33 Discrete CDF of the repair cost distribution for 475 years return period intensity level
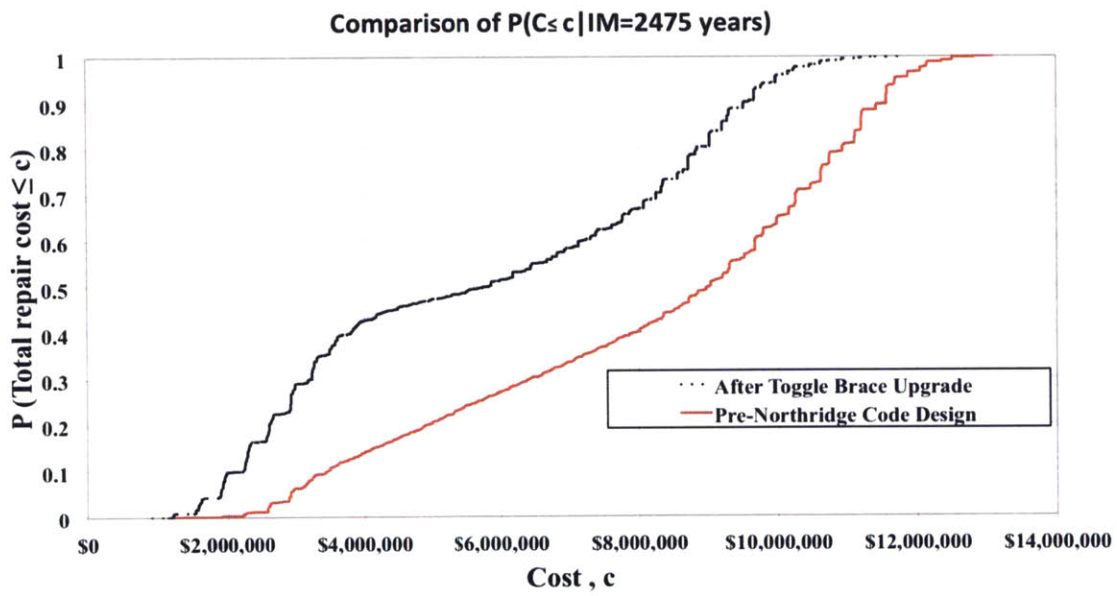
Figure 34 Discrete CDF of the repair cost distribution for 475 years return period intensity level

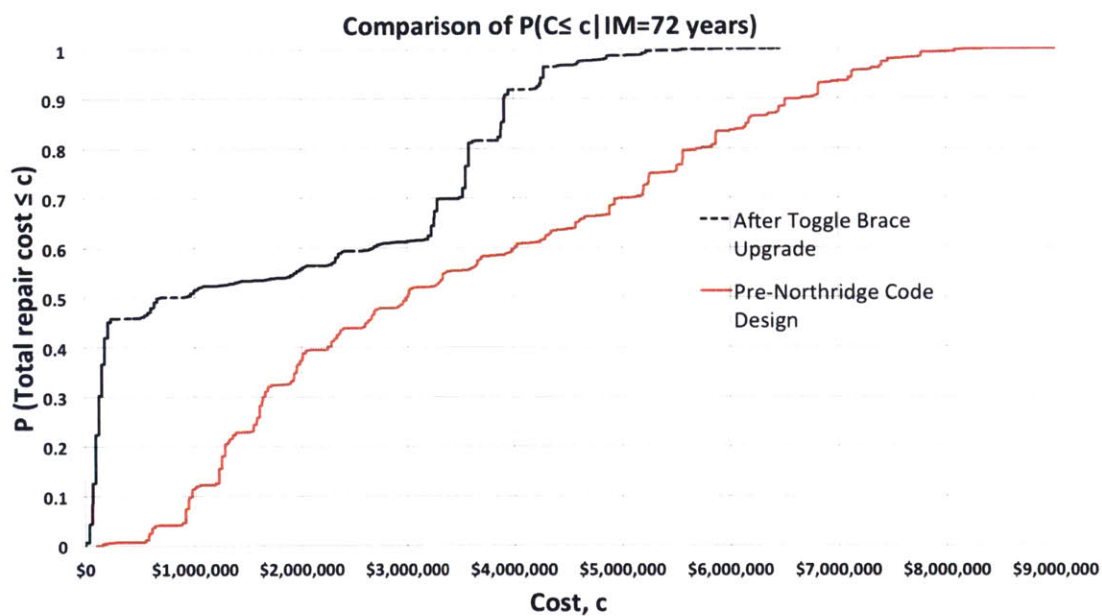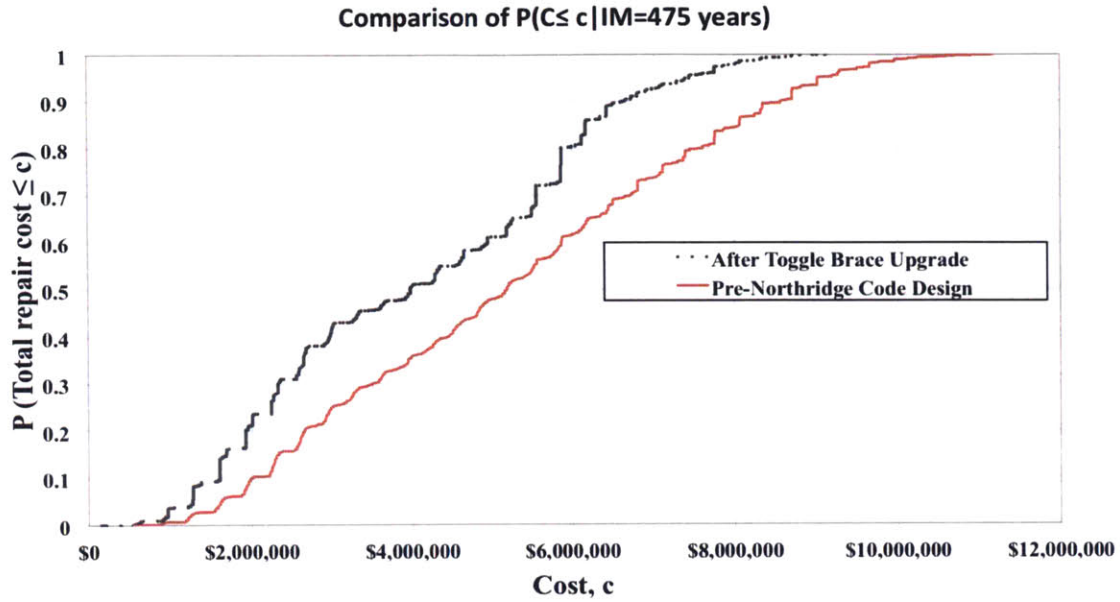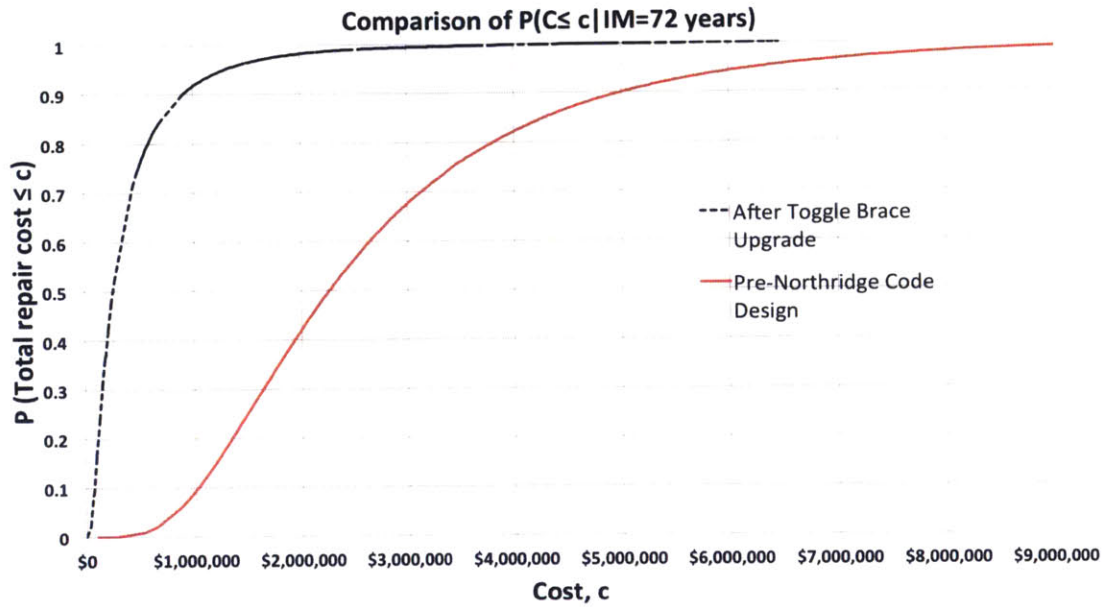**Figure 35 Log-normal CDF of the repair cost distribution for 72 years return period intensity level**
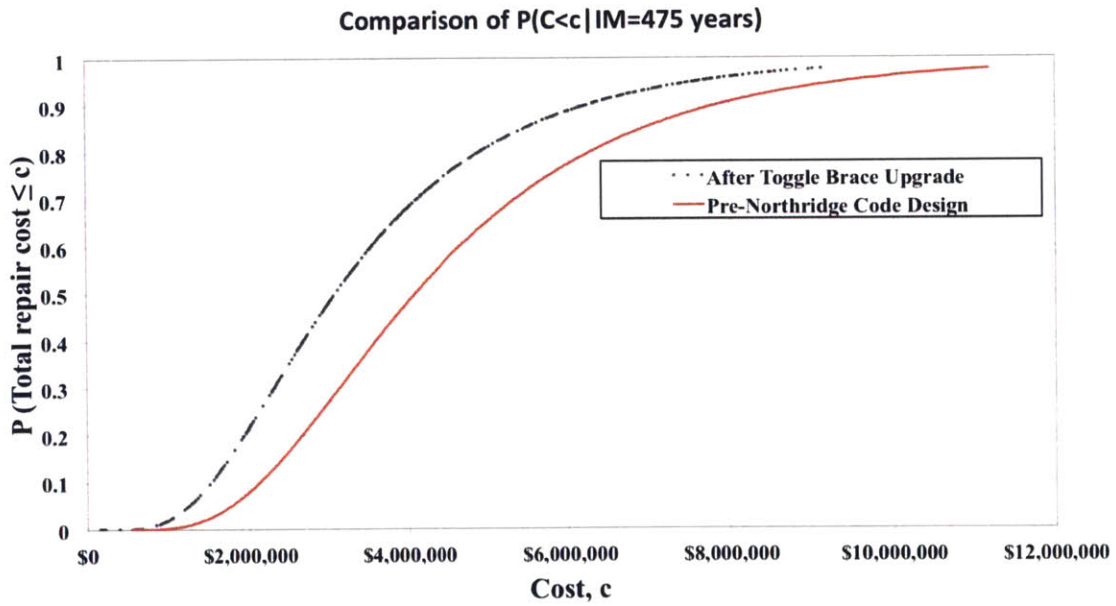
Figure 36 Log-normal CDF of the repair cost distribution for 475 years return period intensity level

Comparison of P(C<c|IM=2475 years)
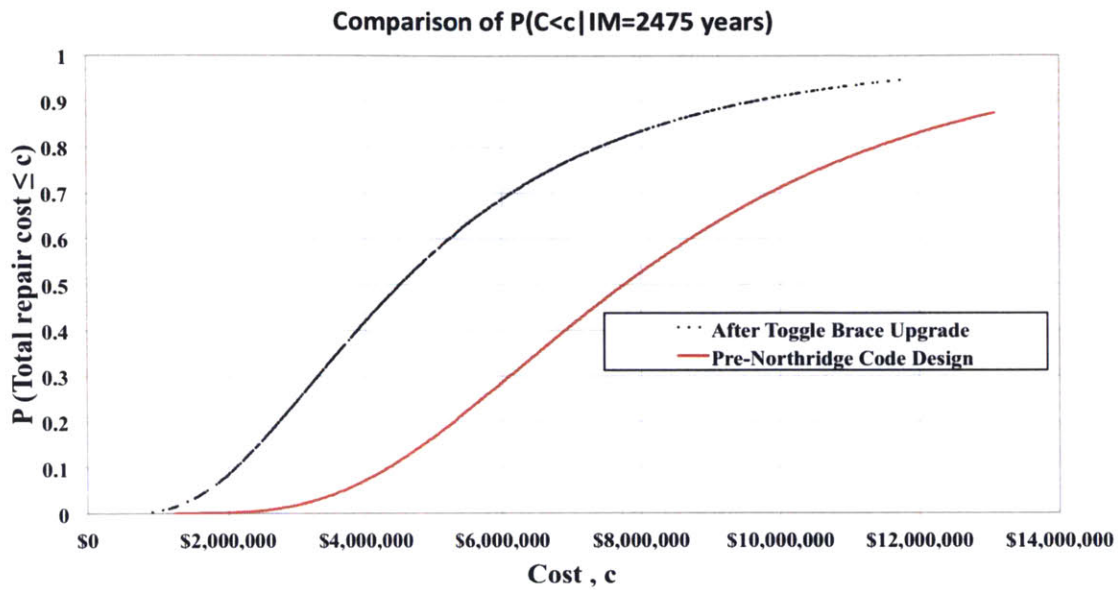
Figure 37 Log-normal CDF of the repair cost distribution for 2475 years return period intensity level

A deaggregation of the total repair cost contributions from each of the performance group is shown in Figure 38 to Figure 43. It is a three dimensional representation of what constitutes of the total repair cost. One example to interpret these three dimensional representation is for 50% probability of exceedance in 50 year hazard level (shown in Figure 38 and Figure 39 for the before and after toggle brace upgrade structures, respectively). The deaggregation in that case indicates that most of the repair cost for the structure before upgrade is concentrated in the interior none-structural, drift sensitive performance groups (INTD12-INTD9R). It is reasonable to interpret this result as, at this seismic hazard level, the none-structure interior items contributes the most to the repair cost, little cost are associate to structural components.

Distribution of repair cost for each performance group(s) - 50/50 before

Figure 38 Deaggregation of the total repair cost for the SAC pre-Northridge frame before toggle brace upgrade at the 50% probability of exceedance in 50 years hazard level

Distribution of repair cost for each performance group(s) - 50/50 after

Figure 39 Deaggregation of the total repair cost for the SAC pre-Northridge frame after toggle brace upgrade at the 50% probability of exceedance in 50 years hazard level

68

Distribution of repair cost for each performance group(s) - 10/50 before
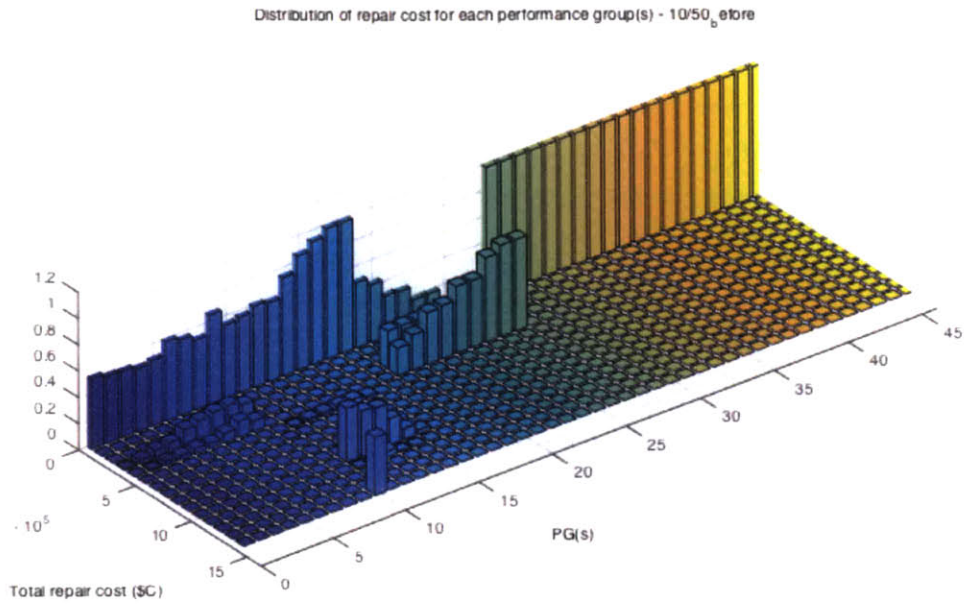
Figure 40 Deaggregation of the total repair cost for the SAC pre-Northridge frame before toggle brace upgrade at the 10% probability of exceedance in 50 years hazard level

Distribution of repair cost for each performance group(s) - 10/50 after

Figure 41 Deaggregation of the total repair cost for the SAC pre-Northridge frame after toggle brace upgrade at the 10% probability of exceedance in 50 years hazard level

69

Distribution of repair cost for each performance group(s) - 2/50 before
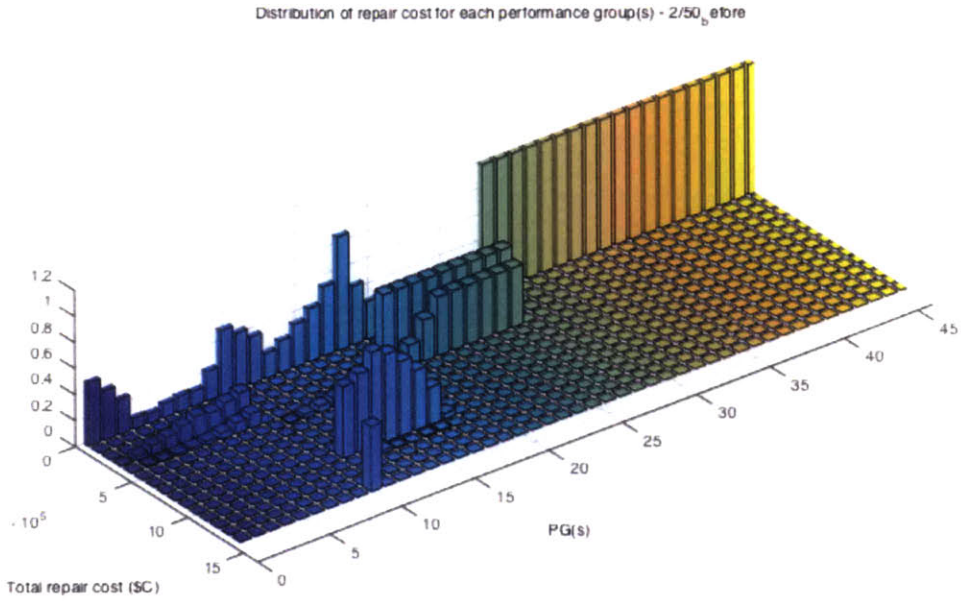
Figure 42 Deaggregation of the total repair cost for the SAC pre-Northridge frame before toggle brace upgrade at the 2% probability of exceedance in 50 years hazard level

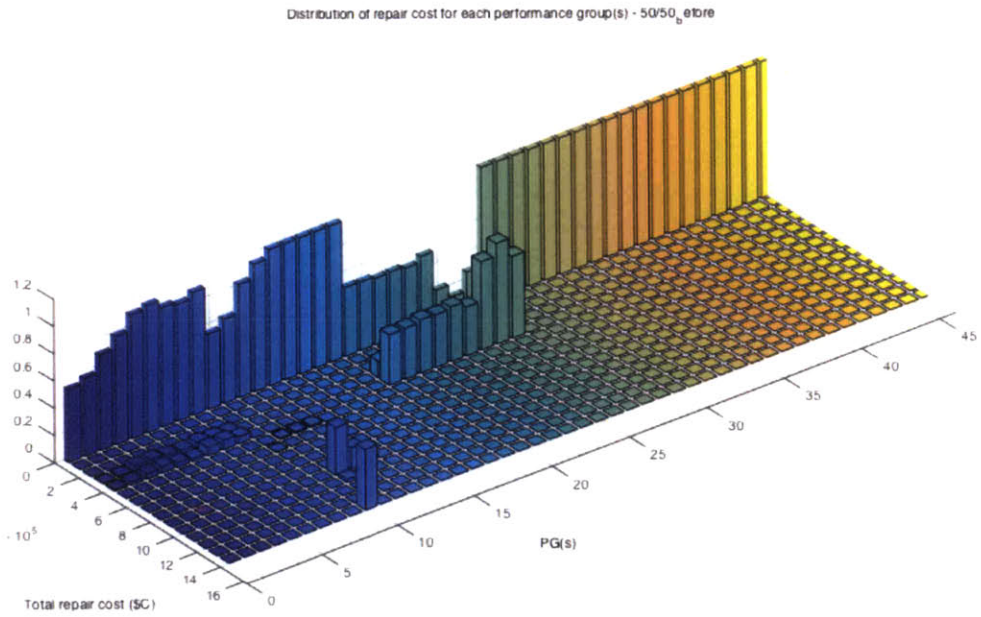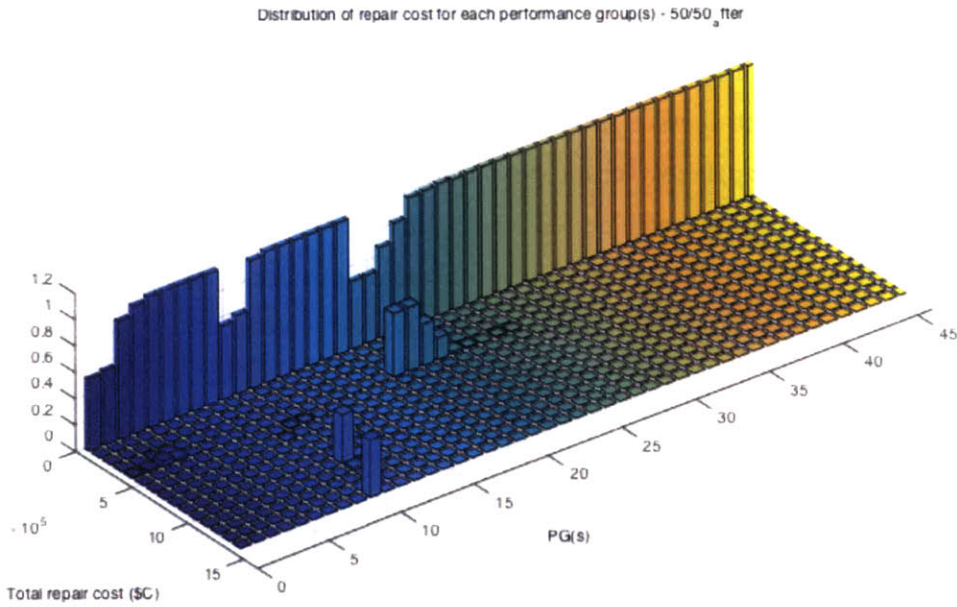Distribution of repair cost for each performance group(s) - 2/50 after
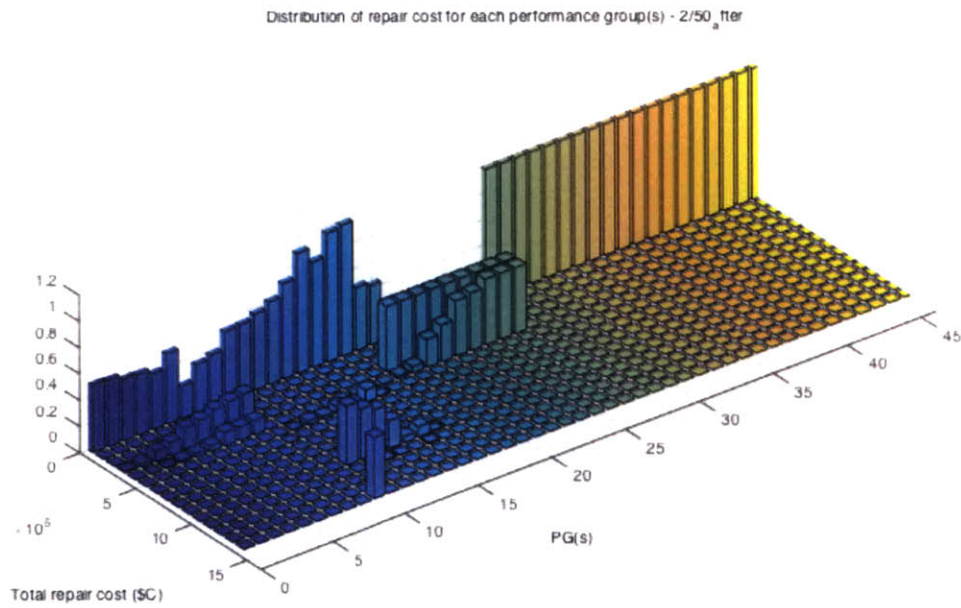
Figure 43 Deaggregation of the total repair cost for the SAC pre-Northridge frame after toggle brace upgrade at the 2% probability of exceedance in 50 years hazard level
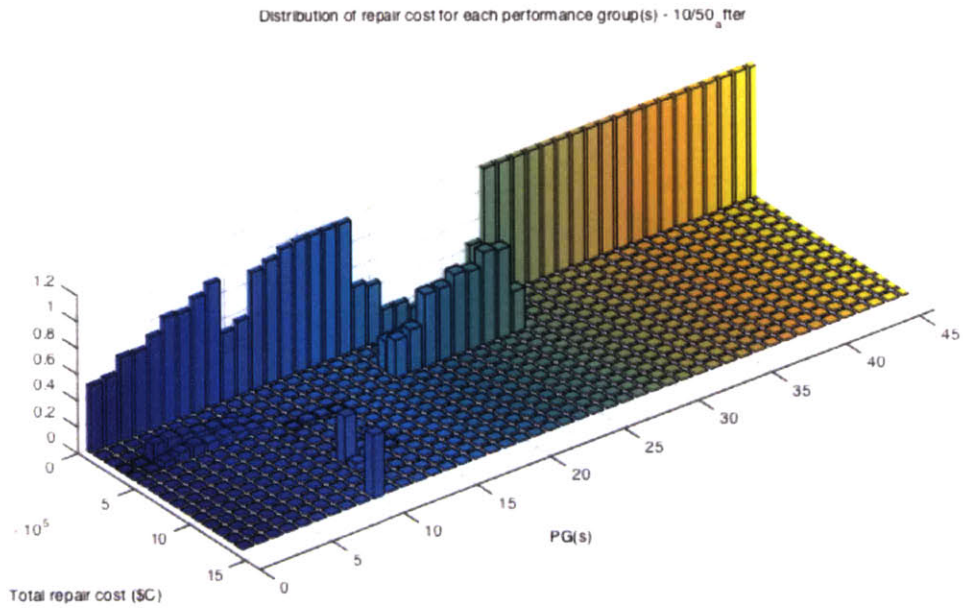
70

CHAPTER 5: SUMMARY AND CONCLUSIONS

There were three research objectives in this thesis. The first objective was to conduct a study of the system behavior of the toggle brace frame. This was accomplished by thorough literature review on toggle brace dampers, and a design procedure is researched for providing the desire damping ratio (12% for this study) for the upgrade of nine-story pre-Northridge design moment frame.

The second objective was to examine how much interstory drift and floor acceleration is reduced in an existing moment frame prototype by adding toggle brace dampers into the system. This was achieved by generating computer models for both before and after toggle brace upgrade of SAC pre-Northridge moment frames. These two models were subjected to three different intensities of ground motion, and their responses were reported in Chapter 4.

The third objective was to develop an implementation of the PEER probabilistic performance-based seismic evaluation of structural framing systems. This was achieved by summarizing the PEER probabilistic performance-based seismic evaluation framework, as presented in Chapter 3. It will enable engineers to quantify performance in terms of capital loss, and thereby help inform decisions about design levels within a risk management framework. This implementation was used to evaluate the performance of the toggle brace frame when they are added to SAC pre-Northridge designed moment frames. The results can be found in Chapter 4.

BIBLIOGRAPHY

Applied Technology Council. (2012). *Seismic Performance Assessment of Buildings Volume 1 - Methodology*. Washington, D.C.: Federal Emergency Management Agency.

Constantinou, M. C., Tsopelas, P., Hammel, W., & Sigaher, A. (2001). Toggle-Brace-Damper Seismic Engergy Dissipation Systems. *Journal of Structural Engineering* (127), 105-112.

Gunay, M., & Mosolam, K. (2012). PEER Performance Based Earthquake Engineering Methodology, Revisited. *15 World Conference Earthquake Engineering* (p. 10). Lisbon: WCEE.

Hunt, J., & Stojadinovic, B. (2010). *Seismic Performance Assessment and Probabilistic Repair Cost Analysis of Precast Concrete Cladding Systems for Multistory Buildings*. Berkeley: Pacific Earthquake Engineering Research Center.

Hwang, J.-S., Huang, Y.-N., Yi, S.-L., & Ho, S.-Y. (2008). Design Formulations for Supplemental Viscous Dampers to Building Structures. *Journal of Structural Engineering* (134), 22-31.

Li, B., & Liang, X. (2008). Seismic Design of Structure With Improved Toggle-Brace-Damper System. *14 WCEE* (pp. 11-0071). Beijing: WCEE.

Mieler, M., Stojadinovic, B., Budnitz, R., Mahin, S., & Comoerio, M. (2013). *Toward Resilient Communities: A Performance-Based Engineering Framework for Design and Evalution of the Built Environment*. Berkeley: Pacific Earthquake Engineering Research Center.

Moehle, J., Stojadinovic, B., Der Kiureghian, A., & Yang, T. (2005). *An Application of PEER Performance-Based Earthquake Engineering Methodology*. University of California, Berkeley. Berkeley: Pacific Earthquake Engineering Research Center.

Raju, K., Prasad, A., Muthumani, K., Gopalakrishnan, N., Iyer, N., & Lakshmanan, N. (2011). Experimental Studies on use of Toggle Brace Mechanism Fitted with Magnetorheological Dampers for Seismic Performance Enhancement of Three-Story Steel Moment-Resisting Frame Model. *Structural Control Health Monitoring* , 373-386.

72

SAC Joint Venture. (2000). *State of the Art Report on Performance prediction and Evaluation of Steel Moment-Frame Buildings.* Los Angeles: Federal Emergency Management Agency.

Yang, T., Moehle, J., & Stojadinovic, B. (2009). *Performance Evaluation of Innovative Steel Braced Frames.* University of California, Berkeley, College of Engineering. Berkeley: Pacific Earthquake Engineering Research Center.

Yang, T., Moehle, J., Stojadinovic, B., & Der Kiureghian, A. (2009). Seismic Performance Evaluation of Facilities: Methodology and Implementation. *Journal of Structural Engineering* , 135-146.

Zhao, Z., & Chan, R. (2014). Parametric Studies of Soft-Storey Structures with Upper Toggle-Brace-Damper Systems. *THE FIRST INTERNATIONAL CONFERENCE ON INFRASTRUCTURE FALIURES AND CONSEQUENCES* (pp. 173-181). Melbourne: CONFERENCE ON INFRASTRUCTURE FALIURES AND CONSEQUENCES.

APPENDIX A: BASIC PROBABILITY THEORY

A.1. INTRODUCTION

To account for uncertainties in earthquake engineering related problems, some prior understanding of basic probability theory is needed. This appendix provided the probability theory that is used in deriving the PBEE methodology. Additional references can be located from any probabilistic and statistics textbooks. One recommended text is the 1.010 lecture notes provided by Professor D. Veneziano from Massachusetts Institute of Technology at Department of Civil and Environmental Engineering (Course 1). Some of the text presented in this appendix is adopted directly from this text.

A.2. BASIC PROBABILITY THEORY

Table A-1 shows a summary of the notations used in this appendix.

Table A- 1 Summary of notations.

Notation	Definition
S	Sample Space. A collection of all possible events.
$\emptyset$	Empty Set. A set contains no events.
E_i	Event i.
$\overline{E}_i$	Complement of event i.
$E_i \cup E_j$	Union of event i and event j.
$E_i E_j \ or \ E_i \cap E_j$	Intersect of event i and event j.

74

$P(E)$	Probability of event i.
$P(E_i\|E_j)$	Conditional probability. Probability of event i given event j.

AXIOMS OF PROBABILITY

Equation of A-1 to Equation A-3 shows the axioms of probability that is used to define the rest of the probability rules.

$$0 \leq P(E_i) \leq 1$$ **Equation A 1**

$$P(S) = 1$$ **Equation A 2**

Event E_i and E_j are said to be mutually exclusive,

$$\text{if } P(E_i \cup E_j) = P(E_i) + P(E_j) \rightarrow P(E_iE_j) = 0 \ for \ i \neq j$$ **Equation A 3**

COLLECTIVE EXCLUSIVE

Event E_i to E_n are said to be collective exclusive, if

$$E_1 \cup E_2 \cup \cdots \cup E_n = S$$ **Equation A 4**

ELEMENTARY RULES OF PROBABILITY

Equation A-5 to Equation A-11 shows some elementary rules of probability. Detail proof can be located from the list of reference.

$$P(E_i \cup E_j) = P(E_i) + P(E_j) - P(E_iE_j)$$ **Equation A 5**

$$P(E_i \cup E_j \cup E_{k)} = P(E_i) + P(E_j) + P(E_k) - P(E_iE_j) - P(E_jE_k)$$
$$- P(E_iE_k) + P(E_iE_jE_k)$$

<div align="right">**Equation A 6**</div>

CONDITIONAL PROBABILITY

$$P(E_i|E_j) = \frac{P(E_iE_j)}{P(E_j)}, if P(E_j) \neq 0$$

<div align="right">**Equation A 7**</div>

$$P(E_1E_2 \cdots E_n) = P(E_1|E_2 \cdots E_n)(E_2|E_3 \cdots E_n) \cdots P(E_n)$$

<div align="right">**Equation A 8**</div>

STATISTICAL INDEPENDENCE

Event E_i and E_j are said to be statistically independent, if

$$P(E_i|E_j) = P(E_i) \Leftrightarrow P(E_j|E_i) = P(E_j)$$

<div align="right">**Equation A 9**</div>

BAYES'S RULE

$$P(E_i|E_j) = P(E_j|E_i)\frac{P(E_i)}{P(E_j)}$$

<div align="right">**Equation A 10**</div>

THEOREM OF TOTAL PROBABILITY

$$P(A) = \sum_{i=1}^{n} P(A|B_i)P(B_i),$$

<div align="right">**Equation A 11**</div>

provided B_i is mutually exclusive and collective exclusive

76

A.3. SINGLE RANDOM VARIABLE

As the number of events in a sample space increases, it is mathematically more challenging to express the probability of each event happening using symbols. Hence, the concept of a single random variable is introduced (concept of multiple random variables will be introduce in Section A.4). A single random variable is defines as a mapping from events in a sample space to numerical values. Each value represents possible outcomes of the sample space. Since the events are mapped into real numbers, formal mathematical equations can be used to deal with the random phenomena. The following example illustrates the concept of random variable.

Example 1: The damage state (DS) of a component in a building after an earthquake can be identified as No Damage (ND), Slight Damage(SD), Moderate Damage(MD) and Heavy Damage(HD). A random variable, X, can be used to represent the damage states of the component, then the possible damage state of the component after an earthquake can be expressed as

$$ND \Rightarrow X = 0$$

$$SD \Rightarrow X = 1$$

$$MD \Rightarrow X = 2$$

$$HD \Rightarrow X = 3$$

At the same time, another random variable, Y, can be used to represent the state of the component With Damage(WD) or No Damage(ND). This means

$$ND \Rightarrow Y = 0$$

$$SD, MD, HD \Rightarrow Y = 1$$

This example illustrates the concept of two separate random variables and their corresponding mapping. Note the mapping of random variable Y is not one-to-one.

PROBABILITY DISTRIBUTION

Once a random variable is defined, the probability of occurrence of each outcome of a random variable can be completely characterized by its probability distribution. The following section defines some of the probability distributions that can be used to characterize a random variable.

If a random variable, X, has discrete outcomes (say $x_1, x_2, \cdots, x_n$), the likelihood of each outcome of the random variable to occur is related to the probability of each event to occur in the original sample space. Hence, a *probability mass function* (PMF), $p_X(x)$, is defined as

$$p_X(x) = P(X = x_i)$$ **Equation A 12**

Since $p_X(x) = 0$ for any $x \neq x_i$ for $i = 1 \cdots n$, PMF must satisfies the following rules

$$0 \leq p_X(x) \leq 1$$ **Equation A 13**

$$\sum_{i=0}^{n} p_X(x_i) = 1$$ **Equation A 14**

If a random variable, X, does not have discrete outcomes, the definition of PMF is not useful to define the probability distribution (since $p_X(x) = 0$ for all x). Hence, a *probability density function* (PDF), $f_X(x)$, is defined for continuous variable. Equation A-15 shows the definition of PDF,

$$\int_{x}^{x+dx} f_X(x)dx = P(x < X \leq x + dx)$$ **Equation A 15**

Similar to PMF, PDF has to satisfy the following rules,

$$0 \leq f_X(x) \qquad\qquad\qquad \text{Equation A 16}$$

$$\int_{-\infty}^{\infty} f_X(x)dx = 1 \qquad\qquad\qquad \text{Equation A 17}$$

Alternatively, the probability distribution of a random variable can be characterized using the *cumulative distribution function* (CDF), $F_X(x)$, where the $F_X(x)$ is defined as

$$F_X(x) = P(X \leq x) = \sum_{x_i \leq x} P_X(x_i)(discrete\ random\ variable) \qquad \text{Equation A 18}$$

$$= \int_{-\infty}^{x} f_X(x)dx\ (continuous\ random\ variable)$$

To ensure the axioms of probability is satisfied, the CDF must satisfy the following rules,

$$F_X(-\infty) = 0\ and\ F_X(\infty) = 1 \qquad\qquad \text{Equation A 19}$$

PARTIAL DESCRIPTORS OF A SINGLE RANDOM VARIABLE

While a probability distribution contains the complete description of a random variable, it is often useful to capture the characteristics of the random variable using partial descriptors. Equation A-20 shows the definition of the nth moment of a random variable and Table A-2 summarized some commonly used partial descriptors and their relation to the nth moment of a random variable.

Definition: the nth moment of random variable, X, is defined as

$$E\{X^n\} = \sum_i x_i^n P_X(x_i)(discrete\ random\ variable) \qquad \text{Equation A 20}$$

$$= \int_{-\infty}^{\infty} x^n f_X(x)dx\ (continuous\ random\ variable)$$

Table A- 2 Commonly used partial descriptor for single random variable, X.

Notation	Descriptions	Equation
Mean μ_X	Average value of X. Also known as the first moment of random variable X.	$\mu_X = E\{X\} = \displaystyle\sum_i x_i P_X(x_i)\ (discrete)$ $= \displaystyle\int_{-\infty}^{\infty} x f_X(x)\ (continuous)$
Median $x_{0.5}$	Value of random variable X, when 50% of the probability lies below and above it.	$F_X(x_{0.5}) = 0.5$
Mode $\tilde{x}$	Value of random variable X, where the outcome has the highest probability.	$P_X(\tilde{x}) = \max\big(P_X(x)\big)\ (discrete)$ $f_X(\tilde{x}) = \max\big(f_X(x)\big)\ (continuous)$
Mean Square $E[x^2]$	Second moment of random variable X.	$E[x^2] = \displaystyle\sum_i x_i^2 P_X(x_i)\ (discrete)$ $= \displaystyle\int_{-\infty}^{\infty} x^2\, f_X(x)dx\ (continuous)$
Variance $Var[X]$	Measure the dispersion of the distribution about its mean. Large value of $Var[X]$ denote large dispersion about the mean.	$Var[X] = \displaystyle\sum_i (x_i - \mu_X)^2 P_X(x_i)\ (discrete)$ $= \displaystyle\int_{-\infty}^{\infty} (x - \mu_X)^2\, f_X(x)dx\ (cont')$ $Note, Var[X] = E[X^2] - (E[X])^2$

Standard deviation σ_X	Square root of the variance. Measure the dispersion of the distribution about its mean. Large value of σ_X denote large dispersion about the mean.	$$\sigma_X = \sqrt{Var[X]}$$
Coefficient of variance δ_X	Normalized measure of dispersion about its mean.	$\delta_X = \frac{\sigma_X}{\lvert\mu_X\rvert}$, Note this only make sense if μ_X is not close to zero.
Third central moment $\mu_{X,3}$	Third central moment of random variable X. Measure the skewness of the distribution about its mean.	$$\mu_{X,3} = \sum_i (x_i - \mu_X)^3 P_X(x_i) \ (discrete)$$ $$= \int_{-\infty}^{\infty} (x - \mu_X)^3 f_X(x)dx \ (cont')$$ $\mu_{X,3} > 0 \Rightarrow Skew \ to \ the \ right \ about \ its \ mean$ $\mu_{X,3} = 0 \Rightarrow Symmetric \ about \ its \ mean$ $\mu_{X,3} < 0 \Rightarrow Skew \ to \ the \ left \ about \ its \ mean$
Coefficient of skewness γ_X	Dimensionless quantity to characterize skewness of the distribution.	$$\gamma_X = \frac{\mu_{X,3}}{\sigma_X^3}$$ $\gamma_X > 0 \Rightarrow Skew \ to \ the \ right \ about \ its \ mean$ $\gamma_X = 0 \Rightarrow Symmetric \ about \ its \ mean$ $\gamma_X < 0 \Rightarrow Skew \ to \ the \ left \ about \ its \ mean$
Coefficient of excess	Measure the flatness of the distribution around its peak.	$$\frac{E[(X - \mu_X)^4]}{\sigma_X^4}$$

A.4. MULTIPLE RANDOM VARIABLES

While section A.3 illustrates the concept of single random variables, most earthquake engineering related problems required concurrent consideration of multiple random variables. This section will summarize the probability distributions and the corresponding partial descriptor for multiple random variables.

A.4.1 PROBABILITY DISTRIBUTION OF MULTIPLE RANDOM VARIABLES

Consider two discrete random variables X and Y, the joint PMF of the random variables is defined as

$$P_{XY}(x,y) = P(X = x_i \cap Y = y_i) \qquad \text{Equation A 21}$$

To satisfy the axioms of probability, the joint PMF of the random variables must satisfy the following rules,

$$0 \leq P_{XY}(x,y) \leq 1 \qquad \text{Equation A 22}$$

$$\sum_i P_{XY}(x_i,y) = P_Y(y) \, and \, \sum_i P_{XY}(x,y_j) = P_X(x) \qquad \text{Equation A 23}$$

$$\sum_i \sum_j P_{XY}(x_i,y_j) = 1 \qquad \text{Equation A 24}$$

If the random variables are continuous, the joint PDF of the random variable is defined as

$$\int_y^{y+dy} \int_x^{x+dx} f_{XY}(x,y)dxdy = P(x < X < x + dx \cap y < Y < y + dy) \qquad \text{Equation A 25}$$

Again, to satisfy the axioms of probability, the joint PDF of the random variables must satisfy the following rules,

$$0 \le f_{XY}(x,y)$$

<div align="right">**Equation A 26**</div>

$$\int_{-\infty}^{\infty} f_{XY}(x,y)dx = f_Y(y) \, and \, \int_{-\infty}^{\infty} f_{XY}(x,y)dy = f_X(x)$$

<div align="right">**Equation A 27**</div>

$$\int_{-\infty}^{\infty} \int_{-\infty}^{\infty} f_{XY}(x,y)dxdy = 1$$

<div align="right">**Equation A 28**</div>

The CDF of the joint random variable is defined as

$$F_{XY}(x,y) = \sum_{y_j \le y} \sum_{x_i \le x} P_{XY}(x_i, y_j) \; (discrete \; random \; variables)$$

<div align="right">**Equation A 29**</div>

$$= \int_{-\infty}^{y} \int_{-\infty}^{x} f_{XY}(x,y)dxdy \; (Continuous \; random \; variables)$$

Similarly, the joint CDF of the random variables must satisfy the following rules

$$F_{XY}(-\infty, \infty) = 0, F_{XY}(x, -\infty) = 0,$$

$$F_{XY}(x, \infty) = F_X(x), F_{XY}(\infty, y) = F_Y(y),$$

<div align="right">**Equation A 30**</div>

$$F_{XY}(\infty, \infty) = 1$$

A.4.2 MOMENTS OF MULTIPLE RANDOM VARIABLES

Like the moments of single random variables, the join moment of multiple random variables provides partial description of the random variables. Table A-3 shows some of the commonly used partial descriptor for two joint random variable X and Y.

Table A- 3 Commonly used partial descriptor for two joint random variables, X and Y.

Notation	Descriptions	Equations
Mean of product $E[XY]$	Mean of the product of random variables X and Y.	$$E[XY] = \sum_j \sum_i x_i\, y_j P_{XY}(x_i, y_j)\, (discrete)$$ $$= \int_{-\infty}^{\infty} \int_{-\infty}^{\infty} xy f_{XY}(x,y)dx, dy\ (continuous)$$
Covariance $Cov[X,Y]$	Joint central moment. $= E[(X - \mu_X)(Y - \mu_Y)]$ Where μ_X and μ_Y are the mean of random variable X and Y respectively.	$$Cov[X,Y] = \sum_j \sum_i (x_i - \mu_X)\left(y_j\right.$$ $$\left. - \mu_Y\right)P_{XY}(x_i, y_j)$$ $(discrete)$ $$= \int_{-\infty}^{\infty} \int_{-\infty}^{\infty} (x - \mu_X)(y - \mu_Y) f_{XY}(x,y)dx, dy$$ $(continuous)$ Note, $Cov[X,Y] = E[XY] - E[X]E[Y]$
Correlation coefficient ρ_{XY}	Dimensionless measure related to covariance. Both covariance and correlation coefficient measure the linear dependence between two random variables.	$$\rho_{XY} = \frac{Cov[X,Y]}{\sigma_X \sigma_Y}, -1 \leq \rho_{XY} \leq 1$$ $\rho_{XY} = \pm 1$ $\Rightarrow Linear\ relation\ between\ X\ and\ Y$ $\rho_{XY} = 0$ $\Rightarrow Complete\ lack\ of\ linear\ dependence$

Table A-3 shows some of the partial descriptor that is commonly used to characterize two joint random variables. If there are more than two random variables, it is more convenient to use matrix notation to present a set of n random variables.

Let $X = [X_1, X_2 \cdots X_n]^T$ be a vector of random variables. The superscript T represents matrix transpose. It is useful to introduce the mean matrix, M_X, and the covariance matrix, Σ_{XX},

$$M_X = \begin{bmatrix} \mu_1 \\ \mu_2 \\ \vdots \\ \mu_n \end{bmatrix} \quad \Sigma_{XX} = \begin{bmatrix} \sigma_1^2 & & & sym \\ Cov[X_2, X_1] & \sigma_2^2 & & \\ \vdots & \vdots & \ddots & \\ Cov[X_n, X_1] & Cov[X_n, X_2] & \cdots & \sigma_n^2 \end{bmatrix} \qquad \text{Equation A 31}$$

Where μ_i and σ_i^2 are the mean and variance of random variable X_i.

In addition, the diagonal matrix of standard deviations, D_X, and the correlation coefficient matrix, R_{XX}, is defined as

$$D_X = \begin{bmatrix} \sigma_1 & 0 & \cdots & 0 \\ 0 & \sigma_2 & & \vdots \\ \vdots & & \ddots & 0 \\ 0 & 0 & \cdots & \sigma_n \end{bmatrix} \quad R_{XX} = \begin{bmatrix} 1 & & & sym \\ \rho_{2,1} & 1 & & \\ \vdots & \vdots & \ddots & \\ \rho_{n,1} & \rho_{n,2} & \cdots & 1 \end{bmatrix} \qquad \text{Equation A 32}$$

Where $\rho_{i,j}$ is the correlation coefficient between random variable X_i and X_j. Using the identify $\rho_{XY} = \frac{Cov[X,Y]}{\sigma_X \sigma_Y}$, one can verify that

$$\Sigma_{XX} = D_X R_{XX} D_X \qquad\qquad \text{Equation A 33}$$

A.5. FUNCTIONS OF RANDOM VARIABLES

Section A.3 and A.4 demonstrates concept of random variables where their probability distribution is known. However in earthquake engineering related problem, the probability distribution of the random variable of interest may not always be easily accessible. For example, the stress level of a

component in a building during an earthquake may not be easily accessible, but can determined in terms of the applied load and building deformation. This section will illustrate the concept of function of random variables where the probability distribution of the dependent random variable can be identified or estimated from independent variables which is accessible.

Let X be a random variable whose probability distribution is known. Let Y be a dependent random variable whose probability distribution depends on the probability distribution of X. If random variable Y can be related to random variable X by a transfer function $Y = g_1(X)$. The nth moment of random variable Y can be calculated using Equation A-34.

$$E\{g_1^n(X)\} = \sum_i g_1^n(x_i)P_X(x_i) \ (discrete \ random \ variable)$$

Equation A 34

$$= \int_{-\infty}^{\infty} g_1^n(x)f_X(x)dx \ (continuous \ random \ variable)$$

Where $P_X(x)$ and $f_X(x)$ are the PMF and PDF of random variable X.